ABSTRACT

BOUNDED BEAM WAVE PULSE PROPAGATION AND SCATTERING IN RANDOM MEDIA BASED ON THE RADIATIVE TRANSFER THEORY USING 2-D GAUSS QUADRATURE FORMULA

by
Sheng-Kai Hu

The scalar time-dependent equation of radiative transfer is used to develop a theory of bounded beam wave narrow band pulse propagation and scattering in a medium characterized by many random discrete scatters, which scatters energy strongly in the forward scattering direction. Applications include the scattering of highly collimated millimeter waves in vegetation and optical beams in the atmosphere. The specific problem analyzed is that of a periodic sequence of Gaussian shaped pulses normally incident from free space onto the planar boundary surface of a random medium half-space, such as a forest, that possesses a scatter (phase) function consisting of a strong, narrow forward lobe superimposed over an isotropic background. After splitting the specific intensity into the reduced incident and diffused intensities, the solution of the transport equation expressed in cylindrical coordinates in the random medium half-space is obtained by using the Fourier-Bessel transform along with the two-dimensional Gauss quadrature formula and an eigenvalue-eigenvector technique, following the procedure developed by Chang and Ishimaru for CW propagation. Curves of received power are obtained for different penetration depths, different incident beamwidths, and different scatter directions. At large penetration depths, as well as for scatter directions different from the incident radiation, the power is shown to attenuate significantly and the pulse widths are shown to broaden, which resulted in considerable pulse distortion. Results for different beam widths are also obtained.

BOUNDED BEAM WAVE PULSE PROPAGATION AND SCATTERING IN RANDOM MEDIA BASED ON THE RADIATIVE TRANSFER THEORY USING 2-D GAUSS QUADRATURE FORMULA

by
Sheng-Kai Hu

A Thesis
Submitted to the Faculty of
New Jersey Institute of Technology
in Partial Fulfillment of the Requirements for the Degree of
Master of Science in Electrical Engineering

Department of Electrical and Computer Engineering

May 2000

Blank Page

APPROVAL PAGE

BOUNDED BEAM WAVE PULSE PROPAGATION AND SCATTERING IN RANDOM MEDIA BASED ON THE RADIATIVE TRANSFER THEORY USING 2-D GAUSS QUADRATURE FORMULA

Sheng-Kai Hu

Dr. Gerald M. Whitman, Thesis Advisor   Date
Professor of Electrical Engineering and Computer Engineering, NJIT

Dr. Edip Niver, Committee Member   Date
Associate Professor of Electrical Engineering and Computer Engineering, NJIT

Dr. Haim Grebel, Committee Member   Date
Professor of Electrical Engineering and Computer Engineering, NJIT

BIOGRAPHICAL SKETCH

Author: Sheng-Kai Hu

Degree: Master of Science

Date: May 2000

Undergraduate and Graduate Education:

- Master of Science in Electrical Engineering,
  New Jersey Institute of Technology, Newark, NJ, 2000

- Attended Master Program of Computer and Information Science
  New Jersey Institute of Technology, Newark, NJ, 1998

- Bachelor of Science in Electrical Engineering
  Yuan-Ze University, Tauyuan, Taiwan, 1993

Major: Electrical Engineering

To my beloved family

ACKNOWLEDGMENT

I would like to express my sincere appreciation to Professor Gerald Whitman for his teaching, guidance, and patient advising during the course of this research. What I have learned from him is not only the materials of this dissertation, but also the insight, concentration, and scrupulosity required to do research. Special thanks are given to Dr. Edip Niver and Dr. Haim Grebel for their actively participating on my thesis committee.

I also wish to thank my parents, Wu-Yi Hu and Ho-Kim Lee for their supporting and encouragement, and my wife Sung-Hee for her understanding and consideration.

TABLE OF CONTENTS

CHAPTER 1

INTRODUCTION

For line-of sight communication, cellular communication in particular, interest centers on the radio-link performance, and how it is affected by wave attenuation, fading and co-channel interference. If vegetation, such as a forest, lies along the path of the link, the radio performance will be affected and, hence, needs to be understood. Since vegetation, a forest, is a medium that is characterized as a random distribution of many discrete scatterers, multiscattering effects play the dominant role affecting the propagation of the radio signal.

Two distinct theories have been developed to deal with multiple scattering effects in random media, namely, analytical multiscattering theory and transport theory [1,2]. In the analytical theory, basic equations such as Maxwell's equations or the wave equation apply. The theory developed is mathematically rigorous, but the solutions that are obtained are approximate and useful in restricted parameter ranges. Transport theory, meanwhile, deals with the transfer of energy through the multiscattering medium. In this theory, the basic equation that is studied is the equation of radiative transfer or the transport equation. This equation is equivalent to Boltzmann's equation in the kinetic theory of gases and in neutron transport theory.

Transport theory developed heuristically from consideration of power and is not as mathematically rigorous as the analytical theory. Nonetheless, transport theory has proven to be successful in the study of many physical problems, such as, optical communication through the atmosphere, millimeter-wave communication links in forests, remote sensing, and radiation from stars. In transport theory, the random medium is characterized by the absorption and scatter cross sections per unit volume, σ_A and σ_S,

1

respectively. And the (power) scatter or phase function $P(\hat{s}, \hat{s}')$, which depends on the incident power unit vector direction $\hat{s}'$ or, equivalently, the angles (θ', ϕ') and the scatter power unit vector direction $\hat{s}$ or, equivalently, the angles (θ, ϕ) for each scatter event (see Figure 1). Over the past several years, a theory of millimeter-wave CW (continuous wave) propagation as well as plane wave pulse propagation in vegetation using transport theory has been developed [3-9]. Of primary interest in these studies was the determination of the range and directional dependency of the received power, as well as pulse broadening and distortion. Pulse broadening is of consequence especially in digital communications where it may cause intersymbol interference and, depending on the data rate, a significant increase in bit error rate.

In the study presented here, the scalar time-dependent equation of radiative transfer is used to develop a theory of beam wave pulse propagation and scattering in a medium that is characterized by many random discrete scatterers which scatter energy strongly in the forward scattering direction. Applications include the scattering of highly collimated millimeter-waves in vegetation and the scattering of optical beams in the atmosphere. Strong forward scattering occurs at millimeter and optical frequencies since all scatter objects in a forest or in the atmosphere are large compared to wavelength. Again of interest are the range and directional dependency of received power, pulse broadening and distortion, in addition to the effect of a finite beamwidth when the incident fields in not a plane wave. Note that the use of the scalar transport equation means that the polarization of the incident beam is not considered, which was justified in [8] by references to experiments performed in vegetation at millimeter-wave frequencies.

The specific problem analyzed here, as depicted in Figure 1, is that of a time periodic sequence of Gaussian pulses normally incident from free space (air) onto a forest region. The forest is modeled as a statistically homogeneous slab or half-space of

randomly distributed particles that scatter and absorb electromagnetic energy. The incident pulse train under investigation is a collimated beam wave, whose intensity variation in the transverse plane is taken to be Gaussian as shown in Figure 1. Since scattering surfaces in a forest have essentially random orientations, it is reasonable to assume that a forest scatters energy symmetrically about the direction of the incident radiation, i.e., that the scattering which occurs at each point in a forest can be characterized by a scatter function that depends only on the angle $\gamma = \cos^{-1}(\hat{s}' \cdot \hat{s})$, which is the angle subtended by the incident direction $\hat{s}'$ and the scatter direction $\hat{s}$, see Figure1. Hence, the scatter function $P(\hat{s},\hat{s}') = P(\hat{s} \cdot \hat{s}') = P(\cos \gamma)$. In addition, since, as noted previously, the forest scatters strongly in the forward direction but minimally in all other direction, the scatter function is assumed to consist of a strong narrow lobe superimposed over an isotropic background. Analytically, such a scatter function can be written in terms of a Gaussian function as follows. (See Figure 2)

$$P(\gamma) \equiv \alpha q(\gamma) + (1-\alpha), \quad q = \left(\frac{2}{\Delta\gamma_s}\right)^2 e^{-(\gamma/\Delta\gamma_s)^2}, \quad \Delta\gamma_s << \pi, \tag{1.1}$$

which is normalized such that

$$\iint\limits_{4\pi} P(\gamma)d\Omega = 4\pi \tag{1.1a}$$

where $d\Omega$ is the differential solid angle about the scatter direction $\hat{s}$, $\Delta\gamma_s$ is the width of the forward lobe of the scatter pattern, and α is the ratio of the forward scattered power to the total scattered power. The scatter function in (1.1) was justified previously in [11] by reference to the theoretical and experimental comparison of results in [8] and [9], and by the experiments conducted by Ulaby et al. in [10].

In transport theory, therefore, according to the above discussion and taking the scatter function to be specified by (1.1), the random scatter medium is characterized by four parameters, namely, σ_A, σ_S, $\Delta\gamma_s$ and α. These four parameters are understood to be "global" parameters in that they remain valid at all points in the random medium and apply to an average scatter event that occurs at every point in the scatter medium.

The approached used to study this beam wave pulse scatter problem is an extension of the method introduced by Chang and Ishimaru in [12] for studying the propagation and scattering of a monochromatic, unpolarized, collimated laser beam with a finite beamwidth in a medium consisting of a random distribution of discrete scatterers. The method of analysis is highly numerical, as no exact analytical solution is available for the case of a beam wave propagating through such a medium.

Chapter 2 develops the scalar equation of radiative transfer in the cylindrical coordinate system. Fourier series representations are introduced for the incident time-periodic pulse train and for all intensity constituents. The incident beam is assumed to be Gaussian and equations for the reduced incident (coherent) and the diffuse (incoherent) intensities are derived, together with appropriate boundary conditions. The Fourier-Bessel transform is used to obtain the equation of transfer for each spatial frequency.

Chapter 3 develops the numerical procedure for solving the transformed transport equation. This involves using the two-dimensional Gauss quadrature formula and an eigenvalue-eigenvector technique.

Chapter 4 presents a re-formulation of the analysis for the special case of a beam-wave pulse train incident on a half-space random medium of discrete scatters rather than a slab.

Chapter 5 presents numerical results for the half-space problem. This includes curves depicting the power received by a highly directive, perfectly matched antenna of narrow beamwidth located in the forest. The curves show pulse spreading and distortion at large penetration depths, the effect on received power of finite incident beamwidths, and the dependence on scatter angle of the received power. In addition, data for the case of an incident periodic sequence of plane wave pulses is used to quantify the accuracy of the numerical procedure used in the beam wave pulse case. This is done two ways. First, the beam wave case is analytically reduced to the plane wave case in order to make a comparison to the data obtained by the completely different analytical approach used in [11]. Secondly, the beam wave result is shown to yield results approaching the plane wave case for large values of beamwidth relative to penetration depth.

Finally, conclusions and possible extensions are discussed in Chapter 6.

CHAPTER 2

TIME-DEPENDENT SCALAR TRANSPORT THEORY

2.1 Equation of Radiative Transfer In The Cylindrical Coordinate System

In its most general form, the scalar time-dependent equation of radiative transfer or transport equation takes the form [13]:

$$\frac{1}{c}\frac{\partial}{\partial t}I(\bar{r},t,\hat{s}) + \hat{s}\cdot\nabla I(\bar{r},t,\hat{s}) = -(\sigma_A + \sigma_S)I(\bar{r},t,\hat{s}) + \frac{\sigma_S}{4\pi}\iint_{4\pi} P(\hat{s},\hat{s}')I(\bar{r},t,\hat{s}')d\Omega',$$

(2.1.1)

where $I(\bar{r},t,\hat{s})$ is the specific intensity which is defined as the power per area and per unit solid angle of the field, at an arbitrary point in the forest at a vector distance $\bar{r}$ from the original and at time t, that flows in the unit vector direction $\hat{s}$; $d\Omega = \sin\theta\ d\phi\ d\theta$ is an element of solid angle with apex at the arbitrary point ; σ_S and σ_A are the scatter and absorption cross-section per unit volume; $P(\hat{s},\hat{s}')$ is the scatter or phase function which describes, for each scatter event, how specific intensity that is incident from a direction $\hat{s}'$ scatters into the direction $\hat{s}$. Implicit in writing (2.1.1) is the assumption that all parameters that describe the scatter medium are independent of frequency. Equation (2.1.1) is rewritten as follows

$$\frac{1}{c}\frac{\partial}{\partial t}I(z,\bar{\rho},t,\hat{s}) + \cos\theta\frac{\partial}{\partial z}I(z,\bar{\rho},t,\hat{s}) + \bar{s}_t\cdot\nabla_t I(z,\bar{\rho},t,\hat{s})$$
$$= -(\sigma_A + \sigma_S)I(z,\bar{\rho},t,\hat{s}) + \frac{\sigma_S}{4\pi}\iint_{4\pi} P(\hat{s},\hat{s}')I(z,\bar{\rho},t,\hat{s}')d\Omega',$$

(2.1.2)

where (see Figure 3)

$$\bar{r} = x\hat{x} + y\hat{y} + z\hat{z} = \rho\hat{\rho} + z\hat{z} \quad , \qquad \hat{s} = \bar{s}_t + \cos\theta\ \hat{z}$$
$$\bar{s}_t = \sin\theta(\cos\phi\ \hat{x} + \sin\phi\ \hat{y}) \quad , \qquad \nabla_t = \frac{\partial}{\partial x}\hat{x} + \frac{\partial}{\partial y}\hat{y} \quad .$$

(2.1.2a)

Introducing (z, ρ, ϕ_x) as the spatial variables of the cylindrical coordinate system and the directional variables (θ, ϕ) for $\hat{s}$, (2.1.2) then becomes

$$\frac{1}{c}\frac{\partial}{\partial t}I(z,\rho,\phi_x,t,\theta,\phi) + (\sigma_A + \sigma_S)I(z,\rho,\phi_x,t,\theta,\phi)$$

$$+ (\cos\theta\frac{\partial}{\partial z} + \sin\theta\cos\phi\frac{\partial}{\partial \rho} + \frac{1}{\rho}\sin\theta\sin\phi\frac{\partial}{\partial \phi_x})I(z,\rho,\phi_x,t,\theta,\phi) \qquad (2.1.3)$$

$$= \frac{\sigma_s}{4\pi}\int_0^{2\pi}\int_0^{\pi} P(\theta,\phi,\theta'\phi')I(z,\rho,\phi_x,t,\theta',\phi')\sin\theta' d\theta' d\phi',$$

where ρ is the radial direction in the (x-y) plane, ϕ_x is the angle between the x-axis and $\bar{\rho}$, θ is the angle between the z-axis and $\hat{s}$, and ϕ is the angle between the x-axis and $\bar{s}_t$ (see Figure 3).

Observe that (2.1.3) depends on six variables. However, for the case being considered here, namely, a normally incident beam wave pulse train and a rotationally symmetric phase function $P(\hat{s},\hat{s}') = P(\hat{s}\cdot\hat{s}')$, a cylindrical symmetry exists about the z-axis. Hence, it can be shown that the equation of radiative transfer (2.1.3) reduces to one which involves the five variables (z, ρ, t, θ, ψ) and is given by [12, 14].

$$\frac{1}{c}\frac{\partial}{\partial t}I(z,\rho,t,\theta,\psi) + (\sigma_A + \sigma_S)I(z,\rho,t,\theta,\psi)$$

$$+ (\cos\theta\frac{\partial}{\partial z} + \sin\theta\cos\psi\frac{\partial}{\partial \rho} - \frac{1}{\rho}\sin\theta\sin\psi\frac{\partial}{\partial \psi})I(z,\rho,t,\theta,\psi) \qquad (2.1.4)$$

$$= \frac{\sigma_s}{4\pi}\int_0^{2\pi}\int_0^{\pi} P(\theta,\psi,\theta'\psi')I(z,\rho,t,\theta',\psi')\sin\theta' d\theta' d\psi',$$

where ψ, defined as the angle between $\bar{\rho}$ and $\bar{s}_t$, is given by (see Figure 4)

$$\bar{s}_t \cdot \bar{\rho} = \rho\sin\theta\cos\psi \qquad (2.1.4a)$$

and $\psi = \phi - \phi_x$, which yields $\dfrac{\partial}{\partial \phi_x} = \dfrac{\partial}{\partial \psi}$ in (2.1.3) equation (2.1.4) is complicated to solve because it involves five independent variables. In the following sections, the Fourier-Bessel transform is used to simplify the above integro-differential equation.

2.2 Fourier Series Representation

The specific intensity of an incident beam wave pulse train traveling through air at the speed of light "c" in the positive z direction is given by

$$I_p = A(\rho)f(t - \frac{z}{c})\frac{\delta(\theta)}{2\pi \sin\theta} \, , \qquad (2.2.1)$$

where the arbitrary but time-periodic pulse train $f(t - z/c)$ with pulse repetition rate T is represented by its Fourier series expansion

$$f(t - \frac{z}{c}) = \text{Re}\left\{\sum_{\upsilon=0}^{\infty} f_\upsilon e^{i\upsilon\omega(t-\frac{z}{c})}\right\} \, , \qquad \omega = \frac{2\pi}{T}, \qquad (2.2.1a)$$

and the amplitude of the beam wave $A(\rho)$ is assumed to dependent on ρ.

Let the bounded beam wave be normally incident upon a slab of finite thickness z_o. Assume that the beam has a Gaussian profile of beamwidth w given by

$$A(\rho) = S_p e^{-(\rho^2 / w^2)}, \qquad (2.2.1b)$$

where S_p is the incident time-averaged Poynting vector at the origin. Thus, the specific intensity of the incident beam wave pulse train takes the form

$$I_p = S_p e^{-(\rho^2 / w^2)} \text{Re}\left\{\sum_{\upsilon=0}^{\infty} f_\upsilon e^{i\upsilon\omega(t-\frac{z}{c})}\right\} \frac{\delta(\theta)}{2\pi \sin(\theta)}. \qquad (2.2.2)$$

As is commonly done [1,15], the specific intensity I is separated into two components, namely, the coherent or reduced incident intensity I_{ri} and the incoherent or diffuse intensity I_d, i.e.,

$$I = I_{ri} + I_d \quad . \qquad (2.2.3)$$

Substituting (2.2.3) into (2.1.4) gives the two equations

$$\frac{1}{c}\frac{\partial}{\partial t}I_{ri} + \frac{\partial}{\partial s}I_{ri} + \sigma_t I_{ri} = 0, \frac{\partial}{\partial s} = \hat{s} \cdot \nabla \qquad (2.2.4a)$$

and

$$\frac{1}{c}\frac{\partial}{\partial t}I_d + \cos\theta\frac{\partial}{\partial z}I_d + \sigma_t I_d + \bar{s}_t \cdot \nabla_t I_d = \frac{\sigma_s}{4\pi}\iint_{4\pi} P(\hat{s},\hat{s}')[I_{ri} + I_d]d\Omega', \qquad (2.2.4b)$$

with the extinction coefficient $\sigma_t = \sigma_A + \sigma_S$ and the term $\bar{s}_t \cdot \nabla_t I_d$ in (2.2.4b) given by the third term on the left side of (2.1.4) excluding the term $\cos\theta \dfrac{\partial}{\partial z} I_d$.

To solve (2.2.4), we introduce the Fourier series representations for the intensities

$$I_j(z,\rho,t,\theta,\psi) = \mathrm{Re}\{\sum_{\upsilon=0}^{\infty} I_{j\upsilon}(z,\rho,\theta,\psi)e^{i\upsilon\omega t}\} \quad , \quad j = p, ri, d \quad , \tag{2.2.5}$$

where $\omega = 2\pi/T$ and T is the time period of the incident pulse train. Note from (2.2.2) that $I_{p\upsilon} = I_{p\upsilon}(z,\rho,\theta)$, i.e., dependents only on z, ρ and θ, which dictates that $I_{ri,\upsilon}$ also depends only on these three variables; hence, only $I_{d\upsilon}$ in (2.2.5) depends on the four variables z, ρ, θ and ψ. Using (2.2.5) reduces (2.2.4) to

$$i\upsilon\frac{\omega}{c} I_{ri,\upsilon} + \frac{\partial}{\partial s} I_{ri} + \sigma_t I_{ri,\upsilon} = 0, \quad \frac{\partial}{\partial s} = \hat{s} \cdot \nabla, \tag{2.2.6a}$$

and

$$i\upsilon\frac{\omega}{c} I_{d\upsilon} + \cos\theta\frac{\partial}{\partial z} I_{d\upsilon} + \sigma_t I_{d\upsilon} + \bar{s}_t \cdot \nabla_t I_{d\upsilon} = \frac{\sigma_s}{4\pi} \iint_{4\pi} P(\hat{s},\hat{s}')[I_{ri,\upsilon} + I_{d\upsilon}]\sin\theta' \, d\theta' d\psi'. \tag{2.2.6b}$$

Because the forest is modeled as a slab of thickness z_o, the boundary conditions that must be satisfied are [1, 12]

$$I_{ri,\upsilon} = I_{p\upsilon} \quad , \quad I_{d\upsilon} = 0 \qquad at \qquad z = 0, \quad 0 \le \theta \le \frac{\pi}{2},$$
$$I_{d\upsilon} = 0 \qquad at \qquad z = z_o \quad \frac{\pi}{2} \le \theta \le \pi. \tag{2.2.7}$$

Equation (2.2.6a) is solved by direct integration and application of the first boundary condition in (2.2.7), which gives

$$I_{ri,\upsilon}(z,\rho,\theta) = S_p f_\upsilon e^{-(\rho^2/w^2)} e^{-\sigma_t z} e^{-i\omega\upsilon z/c} \frac{\delta(\theta)}{2\pi\sin(\theta)}. \tag{2.2.8}$$

Substituting (2.2.8) for $I_{ri,\upsilon}$ in (2.2.6b) yields

$$i\upsilon\frac{\omega}{c}I_{d\upsilon}+\cos\theta\frac{\partial}{\partial z}I_{d\upsilon}+\sigma_t I_{d\upsilon}+\overline{s}_t\cdot\nabla_t I_{d\upsilon}=\frac{\sigma_s}{4\pi}\iint_{4\pi}P(\hat{s},\hat{s}')I_{d\upsilon}(z,\rho,\hat{s}')\sin\theta'\,d\theta'd\psi'+\varepsilon_{ri,\upsilon}\quad,$$

(2.2.9)

where
$$\varepsilon_{ri,\upsilon}=\frac{\sigma_s}{4\pi}\iint_{4\pi}P(\hat{s},\hat{s}')I_{ri,\upsilon}(z,\rho,\theta')\sin\theta'\,d\theta'd\psi'$$
(2.2.9a)

and
$$P(\hat{s},\hat{s}')=P(\theta,\psi,\theta',\psi')\quad.$$
(2.2.9b)

The later identity is written to emphasize that the direction of scatter is defined by the angles θ and ψ as opposed to the usual angle θ and ϕ of the spherical coordinate system. In the discussion to follow, (2.2.9) subject to the boundary conditions in (2.2.7) is solved.

2.3 Fourier-Bessel Transform of the Time-Dependent Transport Equation

To simplify (2.2.9), the Fourier-Bessel transform in the xy-plane and its inverse are used. Let $I_{F\upsilon}$ be the Fourier-Bessel transform of $I_{d\upsilon}$ with respect to $\overline{\rho}$ so that

$$I_{F\upsilon}(z,\overline{k},\hat{s})=\int_0^{2\pi}\int_0^{\infty}I_{d\upsilon}(z,\overline{\rho},\hat{s})e^{i\overline{k}\cdot\overline{\rho}}\,d\overline{\rho}$$
(2.3.1a)

and
$$I_{d\upsilon}(z,\overline{\rho},\hat{s})=\frac{1}{(2\pi)^2}\int_0^{2\pi}\int_0^{\infty}I_{F\upsilon}(z,\overline{k},\hat{s})e^{-i\overline{k}\cdot\overline{\rho}}\,d\overline{k}\ ,$$
(2.3.1b)

where $d\overline{\rho}=\rho\,d\rho\,d\psi$ and $d\overline{k}=k\,dk\,d\psi_k$. Using the above transform it follows that

$$\int_0^{2\pi}\int_0^{\infty}\overline{s}_t\cdot\nabla_t I_{d\upsilon}(z,\overline{\rho},\hat{s})e^{i\overline{k}\cdot\overline{\rho}}\,d\overline{\rho}=-i\overline{k}\cdot\overline{s}_t I_{F\upsilon}(z,\overline{k},\hat{s})\ .$$
(2.3.2)

For convenience, we introduce the normalized variables

$$\tau = \sigma_t z \quad , \quad \tau_\rho = \sigma_t \rho \quad , \quad t' = \sigma_t ct, \tag{2.3.3a}$$

the change in variable

$$\mu = \cos\theta \tag{2.3.3b}$$

and the normalized parameters

$$W_o = \frac{\sigma_s}{\sigma_t} \quad , \quad \omega' = \frac{2\pi}{T'} \quad , \quad T' = \sigma_t cT. \tag{2.3.3c}$$

The parameter W_o is called the albedo.

Using the Fourier-Bessel transform (2.3.1a) and (2.3.2) as well as the changes introduced in (2.3.3) reduce (2.2.9) to the equation

$$(\mu\frac{\partial}{\partial\tau} + 1 + i\omega'\upsilon - i\kappa\sqrt{1-\mu^2}\cos\psi_\kappa)I_{F\upsilon}(\tau,\kappa,\mu,\psi_\kappa)$$

$$= \frac{W_o}{4\pi}\int_{-1}^{1}\int_{0}^{2\pi} P(\mu,\psi_\kappa,\mu',\psi_\kappa')I_{F\upsilon}(\tau,\kappa,\mu',\psi_\kappa')d\psi_\kappa'd\mu' + E_\upsilon(\tau,\kappa,\mu), \tag{2.3.4}$$

where $\bar{\kappa} = \bar{k}/\sigma_t$, ψ_κ is the angle between $\bar{s}_t$ and $\bar{\kappa}$ given by

$\bar{s}_t \cdot \bar{\kappa} = \kappa\sin\theta\cos\psi_\kappa = \kappa\sqrt{1-\mu^2}\cos\psi_\kappa$ (see Figure 4) and $E_\upsilon(\tau,\kappa,\mu)$ is the Fourier-Bessel transform of $\varepsilon_{ri,\upsilon}/\sigma_t$. Note that κ, W_o and υ appear as parameters in (2.3.4) while the equation itself depends on the three variables τ, μ and ψ_κ. In contrast, (2.1.4) depends on five variables z, ρ, t, θ and ψ .

Rewriting the transform pair in (2.3.1) in terms of the normalized quantities defined in (2.3.3) gives

$$I_{F\upsilon}(\tau,\kappa,\mu,\psi_\kappa) = \frac{1}{\sigma_t^2}\int_{0}^{2\pi}\int_{0}^{\infty} I_{d\upsilon}(\tau,\tau_\rho,\mu,\psi)e^{i\kappa\tau_\rho\cos(\psi-\psi_\kappa)}\tau_\rho d\tau_\rho d\psi, \tag{2.3.5a}$$

$$I_{d\upsilon}(\tau,\tau_\rho,\mu,\psi) = \frac{\sigma_t^2}{(2\pi)^2}\int_{0}^{2\pi}\int_{0}^{\infty} I_{F\upsilon}(\tau,\kappa,\mu,\psi_\kappa)e^{-i\kappa\tau_\rho\cos(\psi-\psi_\kappa)}\kappa \, d\kappa \, d\psi_\kappa \quad . \tag{2.3.5b}$$

2.4 The Fourier-Bessel Transform of the Source Function $\varepsilon_{ri,\upsilon}$

Converting (2.2.8) to normalized variables, the reduced incident specific intensity takes the form

$$I_{ri,\upsilon}(\tau,\tau_p,\theta) = S_p f_\upsilon e^{-(\tau_p/\sigma_t w)^2} e^{-\eta_\upsilon \tau} \frac{\delta(\theta)}{2\pi\sin(\theta)} \quad , \qquad (2.4.1)$$

where

$$\eta_\upsilon = 1 + i\upsilon\omega' \quad . \qquad (2.4.1a)$$

The source function generated by $I_{ri,\upsilon}$ as defined in (2.2.9a) is determined by using (2.4.1), which gives

$$\begin{aligned}
\frac{\varepsilon_{ri,\upsilon}(\tau,\tau_p,\theta)}{\sigma_t} &= \frac{W_o}{4\pi} \int_0^{2\pi}\int_0^{\pi} S_p f_\upsilon e^{-(\tau_p/\sigma_t w)^2} e^{-\eta_\upsilon \tau} \frac{\delta(\theta')}{2\pi\sin(\theta')} P(\theta,\psi,\theta',\psi')\sin\theta' d\theta' d\psi' \\
&= \frac{W_o}{4\pi} S_p f_\upsilon e^{-(\tau_p/\sigma_t w)^2} e^{-\eta_\upsilon \tau} P(\mu) \quad .
\end{aligned}$$

$$(2.4.2)$$

This result is obtained by assuming the scattering to be symmetric about the direction of the incident wave, i.e., $P(\hat{s},\hat{s}') = P(\hat{s}\cdot\hat{s}')$. Note that

$$\hat{s}\cdot\hat{s}' \equiv \cos\gamma = \mu\mu' + \sqrt{1-\mu^2}\sqrt{1-\mu'^2}\cos(\psi-\psi') \qquad (2.4.3)$$

with $\mu = \cos\theta$, $\mu' = \cos\theta'$, from which it follows that $P(\hat{s}\cdot\hat{s}') = P(\mu)$ when $\theta' = 0°$ ($\mu' = 1$).

From (2.3.5a), the Fourier-Bessel transform of the source function $\varepsilon_{ri,\mu}(\tau,\tau_p,\mu)$ in (2.4.2) is found to be

$$E_\upsilon(\tau,\kappa,\mu) = \frac{1}{\sigma_t^2} \int_0^{2\pi}\int_0^{\infty} \frac{\varepsilon_{ri,\mu}(\tau,\tau_p,\mu)}{\sigma_t} e^{i\kappa\tau_p \cos(\psi-\psi_\kappa)} \tau_p d\tau_p d\psi \quad . \qquad (2.4.4)$$

Using the following identities [16]

$$\int_0^{2\pi} e^{i\kappa\tau_p \cos(\psi-\psi_\kappa)} d\psi = 2\pi J_o(\kappa\tau_p) \qquad (2.4.5a)$$

$$\int_0^{\infty} e^{-a^2 x^2} J_n(bx) x^{n+1} dx = \frac{b^n}{(2a^2)^{n+1}} e^{-(b^2/4a^2)} \qquad (2.4.5b)$$

and substituting (2.4.2) into (2.4.4) yields

$$E_v(\tau,\kappa,\mu) = \frac{1}{\sigma_t^2}\frac{W_o}{4\pi} S_p f_v \int_0^\infty \int_0^{2\pi} e^{-(\tau_\rho/\sigma_t w)^2} e^{-\eta_v \tau} P(\mu)\, e^{i\kappa\tau_\rho \cos(\psi-\psi_\kappa)} d\psi\, \tau_\rho d\tau_\rho$$

$$= \frac{1}{\sigma_t^2}\frac{W_o}{2} S_p f_v e^{-\eta_v \tau} P(\mu)\int_0^\infty e^{-(\tau_\rho/\sigma_t w)^2} J_o(\kappa\tau_\rho)\tau_\rho d\tau_\rho$$

$$= \frac{W_o}{4\pi} S_p f_v A_w e^{-\eta_v \tau} P(\mu) e^{-\kappa^2/\kappa_o^2} \quad,$$

$$(2.4.6)$$

where $J_o(\kappa\tau_\rho)$ is the zero order Bessel function and

$$\kappa_o = \frac{2}{\sigma_t w} \qquad , \qquad A_w = \pi w^2 . \qquad (2.4.6a)$$

Since the spatial spectrum in (2.4.6) decreases as $e^{-\kappa^2/\kappa_o^2}$, the constituents with $\kappa > \kappa_o$ are small. Hence, the constituents with $\kappa < \kappa_o$ contribute most significantly to the final beam solution when (2.3.5b) is used to find I_{dv} [12].

CHAPTER 3

2-D QUADRATURE METHOD OF SOLUTION TO THE TIME-DEPENDENT TRANSPORT EQUATION

In the previous chapter, the Fourier-Bessel transform was used to obtain the transformed transport equation given in (2.3.4) along with (2.4.6). In the present chapter, this transformed transport equation, subjected to appropriate boundary conditions, is solved numerically using the method presented in [12], which will be referred to as the discrete ordinate method using the 2-dimensional quadrature formula or, simply, the 2-D quadrature method. The method in [12] was developed to treat the time-independent transport equation for the beam wave problem. As expected, the time-dependent case is more complicated. It is shown below that the complementary solution to the pertinent system of differential equations remains formally the same as in [12] but that the particular solution is different. The solution reduces properly to the time-independent case ($\upsilon = 0$).

3.1 Mathematical Description of the Bounded Beam

The transformed transport equation (2.3.4) with the source function $E_\upsilon(\tau,\kappa,\mu)$ given in (2.4.6) is rewritten more conveniently as

$$(\mu \frac{\partial}{\partial \tau} - i\kappa\sqrt{1-\mu^2}\cos\psi_\kappa)I_{F\upsilon}(\tau,\kappa,\mu,\psi_\kappa) = -\eta_\upsilon I_{F\upsilon}(\tau,\kappa,\mu,\psi_\kappa)$$

$$+ \frac{W_o}{4\pi} \int_{-1}^{1}\int_{0}^{2\pi} P(\mu,\psi_\kappa,\mu',\psi_\kappa')I_{F\upsilon}(\tau,\kappa,\mu',\psi_\kappa')d\psi_\kappa'd\mu' \qquad (3.1.1)$$

$$+ \frac{W_o}{4\pi}S_p f_\upsilon A_w e^{-\eta_\upsilon \tau}P(\mu)e^{-\kappa^2/\kappa_o^2} \quad ,$$

where $\eta_\upsilon = 1 + i\upsilon\omega'$, $A_w = \pi w^2$ and $\kappa_o = 2/\sigma_t w$.

Taking the Fourier-Bessel transform of the boundary conditions in equation (2.2.7) gives

$$I_{F\upsilon}(\tau = 0,\kappa,\mu,\psi_\kappa) = 0 \ for \quad 0 \le \mu \le 1 \ , \quad 0 \le \psi_\kappa < 2\pi$$

$$I_{F\upsilon}(\tau = \tau_o,\kappa,\mu,\psi_\kappa) = 0 \ for \ -1 \le \mu \le 0 \ , \quad 0 \le \psi_\kappa < 2\pi \qquad (3.1.1a)$$

14

Equation (3.1.1) together with the boundary conditions in (3.1.1a) constitute the complete mathematical description of the transformed diffuse intensity for the time-dependent bounded beam problem. Because of the term $\cos\psi_\kappa$, the solution to (3.1.1) is an even function of the variable ψ_κ, i.e.,

$$I_{F\upsilon}(\tau,\kappa,\mu,\psi_\kappa) = I_{F\upsilon}(\tau,\kappa,\mu,-\psi_\kappa) \quad . \tag{3.1.2}$$

This allows the integral in (3.1.1) to take the form

$$\int_{-1}^{1}\int_{0}^{2\pi} P(\mu,\psi_\kappa,\mu',\psi_\kappa')I_{F\upsilon}(\tau,\kappa,\mu',\psi_\kappa')d\psi_\kappa'd\mu'$$

$$= \int_{-1}^{1}\int_{0}^{\pi} \{P(\mu,\psi_\kappa,\mu',\psi_\kappa') + P(\mu,\psi_\kappa,\mu',-\psi_\kappa')\}I_{F\upsilon}(\tau,\kappa,\mu',\psi_\kappa')d\psi_\kappa'd\mu' \quad . \tag{3.1.3}$$

Let $I_{F\upsilon}$ be written as a sum of real and imaginary functions:

$$I_{F\upsilon}(\tau,\kappa,\mu,\psi_\kappa) = I_{F,a\upsilon}(\tau,\kappa,\mu,\psi_\kappa) + iI_{F,b\upsilon}(\tau,\kappa,\mu,\psi_\kappa) \quad . \tag{3.1.4}$$

Due to the symmetry property of $I_{F\upsilon}(\tau,\kappa,\mu,\psi_\kappa)$ in (3.1.2), these real and imaginary functions satisfy the relations

$$I_{F,a\upsilon}(\tau,\kappa,\mu,\psi_\kappa) = I_{F,a\upsilon}(\tau,\kappa,\mu,-\psi_\kappa) \tag{3.1.5a}$$

and

$$I_{F,b\upsilon}(\tau,\kappa,\mu,\psi_\kappa) = I_{F,b\upsilon}(\tau,\kappa,\mu,-\psi_\kappa) \quad . \tag{3.1.5b}$$

Substituting (3.1.4) into (3.1.1) yields:

$$(\mu\frac{\partial}{\partial\tau} - i\kappa\sqrt{1-\mu^2}\cos\psi_\kappa)(I_{F,a\upsilon} + iI_{F,b\upsilon}) = -\eta_\upsilon(I_{F,a\upsilon} + iI_{F,b\upsilon})$$

$$+ \frac{W_o}{4\pi}\int_{-1}^{1}\int_{0}^{2\pi} P(\mu,\psi_\kappa,\mu',\psi_\kappa')(I_{F,a\upsilon} + iI_{F,b\upsilon})d\psi_\kappa'd\mu' \tag{3.1.6}$$

$$+ \frac{W_o}{4\pi}S_p f_\upsilon A_w e^{-\eta_\upsilon\tau}P(\mu)e^{-\kappa^2/\kappa_o^2} \quad .$$

Replacing η_υ by its real and imaginary parts allows the exponential term to be expressed also in terms of real and imaginary parts:

$$e^{-\eta_\upsilon\tau} = e^{-(1+i\omega'\upsilon)\tau} = e^{-\tau}[\cos(\omega'\upsilon\tau) - i\sin(\omega'\upsilon\tau)] \quad . \tag{3.1.7}$$

Equation (3.1.6) is then separated into real and imaginary terms. Using (3.1.3), (3.1.5a,b) and (3.1.7), the following coupled differential equations are obtained

$$\mu\frac{\partial}{\partial\tau}I_{F,a\upsilon}(\tau,\kappa,\mu,\psi_{\kappa}) = -[\kappa\sqrt{1-\mu^2}\cos\psi_{\kappa} - \omega'\upsilon]I_{F,b\upsilon}(\tau,\kappa,\mu,\psi_{\kappa}) - I_{F,a\upsilon}(\tau,\kappa,\mu,\psi_{\kappa})$$

$$+\frac{W_o}{4\pi}\int_{-1}^{1}\int_{0}^{\pi}P_S(\mu,\psi_{\kappa},\mu',\psi_{\kappa}')I_{F,a\upsilon}(\tau,\kappa,\mu',\psi'_{\kappa})d\psi_{\kappa}'d\mu'$$

$$+\frac{W_o}{4\pi}S_p f_\upsilon A_w P(\mu)e^{-\kappa^2/\kappa_o^2}e^{-\tau}\cos(\omega'\upsilon\tau)$$

(3.1.8a)

and

$$\mu\frac{\partial}{\partial\tau}I_{F,b\upsilon}(\tau,\kappa,\mu,\psi_{\kappa}) = [\kappa\sqrt{1-\mu^2}\cos\psi_{\kappa} - \omega'\upsilon]I_{F,a\upsilon}(\tau,\kappa,\mu,\psi_{\kappa}) - I_{F,b\upsilon}(\tau,\kappa,\mu,\psi_{\kappa})$$

$$+\frac{W_o}{4\pi}\int_{-1}^{1}\int_{0}^{\pi}P_S(\mu,\psi_{\kappa},\mu',\psi_{\kappa}')I_{F,b\upsilon}(\tau,\kappa,\mu',\psi'_{\kappa})d\psi_{\kappa}'d\mu'$$

$$-\frac{W_o}{4\pi}S_p f_\upsilon A_w P(\mu)e^{-\kappa^2/\kappa_o^2}e^{-\tau}\sin(\omega'\upsilon\tau) \quad,$$

(3.1.8b)

where $$P_S(\mu,\psi_{\kappa},\mu',\psi_{\kappa}') = P_I(\xi,\xi') + P_{II}(\xi,\xi')$$ (3.1.9)

with $$P_I(\xi,\xi') = P(\mu,\psi_{\kappa},\mu',\psi_{\kappa}'), \quad P_{II}(\xi,\xi') = P(\mu,\psi_{\kappa},\mu',-\psi_{\kappa}').$$ (3.1.10)

$P_I(\xi,\xi')$ represents the phase function in the 1st and 2nd quadrants (east hemisphere) and $P_{II}(\xi,\xi')$ represents the phase function in the 3rd and 4th quadrants (west hemisphere) as ψ'_{κ} varies from 0 to π.

To simplify (3.1.1) and (3.1.8a,b), we introduce the new variables $I_{a\upsilon}$ and $I_{b\upsilon}$ such

that $$I_{F,x\upsilon} = S_p f_\upsilon A_w e^{-\kappa^2/\kappa_o^2}I_{x\upsilon} \quad, \quad where \quad x = a,b \ ,$$ (3.1.11)

to obtain the two normalized coupled equations:

$$\mu \frac{\partial}{\partial \tau} I_{a\upsilon}(\tau, \kappa, \mu, \psi_\kappa) = -[\kappa \sqrt{1-\mu^2} \cos\psi_\kappa - \omega'\upsilon] I_{b\upsilon}(\tau, \kappa, \mu, \psi_\kappa) - I_{a\upsilon}(\tau, \kappa, \mu, \psi_\kappa)$$

$$+ \frac{W_o}{4\pi} \int_{-1}^{1}\int_{0}^{\pi} P_S(\mu, \psi_\kappa, \mu', \psi_\kappa') I_{a\upsilon}(\tau, \kappa, \mu', \psi'_\kappa) d\psi_\kappa' d\mu'$$

$$+ \frac{W_o}{4\pi} P(\mu) e^{-\tau} \cos(\omega'\upsilon\tau)$$

$$(3.1.12a)$$

$$\mu \frac{\partial}{\partial \tau} I_{b\upsilon}(\tau, \kappa, \mu, \psi_\kappa) = [\kappa \sqrt{1-\mu^2} \cos\psi_\kappa - \omega'\upsilon] I_{a\upsilon}(\tau, \kappa, \mu, \psi_\kappa) - I_{b\upsilon}(\tau, \kappa, \mu, \psi_\kappa)$$

$$+ \frac{W_o}{4\pi} \int_{-1}^{1}\int_{0}^{\pi} P_S(\mu, \psi_\kappa, \mu', \psi_\kappa') I_{b\upsilon}(\tau, \kappa, \mu', \psi'_\kappa) d\psi_\kappa' d\mu'$$

$$- \frac{W_o}{4\pi} P(\mu) e^{-\tau} \sin(\omega'\upsilon\tau) \quad .$$

$$(3.1.12b)$$

In (3.1.12a) and (3.1.12b), the most difficult task is to evaluate the integral terms. Chang and Ishimaru [12] chose to use the 2-D Gauss quadrature formula, which approximates the integral terms as finite summations. The same technique is used here. A description of the method is presented in Appendix A.

3.2 2-D Gauss Quadrature Formula

Since an analytical solution to (3.1.1) is not available, a numerical approach to the bounded beam problem is employed. As in [12], the coupled integro-differential equation is converted to a system of differential equations that are solved numerically. To approximate the integral terms, use is made of the 2-D Gauss quadrature formula. As noted above, the solution to (3.1.1) is an even function in the variable ψ_κ. The problem is then divided into two regions of space, namely, the east and west hemisphere. Because of symmetry, the problem need only be solved in one of these regions. The east hemisphere is chosen, which is defined as

$$0 \le \theta \le \pi \, , \, 0 \le \psi_\kappa \le \pi \quad .$$

$$(3.2.1)$$

The problem does not have the additional symmetry properties used in [12]. The method of solution is the same, except that more terms are needed to evaluate the integral.

To approximate the double integrations, the following changes in variables are introduced

$$\mu = \cos\theta \quad \text{and} \quad \alpha = \cos\psi_\kappa \qquad (3.2.2)$$

and the Gauss-Chebyshev and Gauss-Legendre formulas are used to yield

$$\int_0^\pi \int_0^\pi h(\theta, \psi_\kappa) \sin\theta \, d\psi_\kappa \, d\theta = \int_{-1}^1 \int_{-1}^1 \frac{h(\mu, \alpha)}{\sqrt{1-\alpha^2}} \, d\alpha \, d\mu$$

$$\approx \sum_{\substack{i=-N_l \\ i\neq 0}}^{N_l} w_i^l \sum_{j=1}^{N_c^i} w_{i,j}^c h(\mu_i^l, \psi_{\kappa(i,j)}^c) \quad , \qquad (3.2.3)$$

where the quadrature points and weights are given by[*]:

$$\theta_{\pm i}^l = \cos^{-1}(\mu_{\pm i}^l) \quad , \quad \psi_{\kappa(i,j)}^c = [\frac{(2j-1)\pi}{2N_c^i}] = \cos^{-1}(\alpha_{i,j}^c), \qquad (3.2.4a)$$

$$w_i^l = \frac{2}{(1-\mu_i^2) P_m'(\mu_i)^2} \quad , \quad w_{i,j}^c = \frac{\pi}{N_c^i} \quad . \qquad (3.2.4b)$$

$P_m(\mu)$ is the mth Legendre polynomial, μ_i is the ith zero of $P_m(\mu)$, and $P_m'(\mu)$ is the derivative of the Legendre polynomial. Further details on the 2-D Gaussian quadrature technique are found in Appendix A.

To simplify the expressions for the numerical approximation of the integrals in (3.1.12), denote ξ as the spherical variable pair (μ, α) and define $d\xi = \frac{d\mu \, d\alpha}{\sqrt{1-\alpha^2}}$. The integral terms in (3.1.12) then take the form:

$$\int_{2\pi} P_S(\xi, \xi') I_{x\upsilon}(\tau, \kappa, \xi') d\xi' \approx \sum_{\substack{q=-N \\ q\neq 0}}^N w_q P_S(\xi, \xi_q) I_{x\upsilon}(\tau, \kappa, \xi_q) \quad . \qquad (3.2.5)$$

---

[*] The value $\mu_{+i}^l (\equiv \cos\theta_{+i}^l)$, $i = 1, \cdots, N$ are defined for angles $0° < \theta_{+i}^l < 90°$ so that $0 < \mu_{+i}^l < 1$, $i > 0$ whereas the values of $\mu_{-i}^l (\equiv \cos\theta_{-i}^l)$, $i = 1, \cdots, N$ are defined for angles $90° < \theta_{-i}^l < 180°$ so that $-1 < \mu_{-i}^l < 0$, $i > 0$. Thus, $\mu_{+i}^l = -\mu_{-i}^l$, $i > 0$.

The single index q that is used in (3.2.5) is defined as follows

$$q = \pm k \quad , \quad (\pm n, m) \rightarrow \pm k \quad , \quad k = \sum_{i=1}^{n-1} N_c^i + m \quad , \tag{3.2.5a}$$

where n, m, k are non-zero integers and

$$N = \sum_{i=1}^{N_l} N_c^i = N_l N_c \quad . \tag{3.2.5b}$$

In (3.2.5b) the last equality holds provided $N_c^i = N_c$. In the reduced k notation, the quadrature points and their weights are given by

$$\xi_{\pm k} = (\mu_{\pm k}, \alpha_{\pm k}) = (\mu_{\pm n}^l, \alpha_{\pm n,m}^c) \quad , \quad w_{\pm k} = w_{\pm n}^l \, w_{\pm n,m}^c \quad . \tag{3.2.5c}$$

With the reduced notation, the specific intensities are discretized in the following manner

$$\bar{I}_{x\upsilon}(\tau, \kappa, \xi_{\pm k}) = \begin{bmatrix} I_{x\upsilon}(\tau, \kappa, \xi_1) \\ \vdots \\ I_{x\upsilon}(\tau, \kappa, \xi_N) \\ I_{x\upsilon}(\tau, \kappa, \xi_{-1}) \\ \vdots \\ I_{x\upsilon}(\tau, \kappa, \xi_{-N}) \end{bmatrix} = \begin{bmatrix} I_{x\upsilon}(\tau, \kappa, \mu_1, \alpha_{1,1}) \\ \vdots \\ I_{x\upsilon}(\tau, \kappa, \mu_1, \alpha_{1,N_c^l}) \\ I_{x\upsilon}(\tau, \kappa, \mu_2, \alpha_{2,1}) \\ \vdots \\ I_{x\upsilon}(\tau, \kappa, \mu_2, \alpha_{2,N_c^l}) \\ \vdots \\ I_{x\upsilon}(\tau, \kappa, \mu_{-N}, \alpha_{-1,1}) \\ \vdots \\ I_{x\upsilon}(\tau, \kappa, \mu_{-N}, \alpha_{-N_l,N_c^l}) \end{bmatrix} \quad . \tag{3.2.6}$$

Note the ordering of the discrete points in the above formulation.

3.3 The Linear System

Using the above discretization, the two coupled integro-differential equations (3.1.12) are converted into a system of 2N differential equations. Substitution of (3.2.5) into (3.1.12) and evaluating at the discrete points $\xi = \xi_i$, $i = \pm k = \pm 1, \pm 2, \cdots \pm N$ gives[*]

$$\mu_i \frac{d}{d\tau} I_{a\upsilon}(\tau, \xi_i) = -I_{a\upsilon}(\tau, \xi_i) - \kappa_{i\upsilon} I_{b\upsilon}(\tau, \xi_i) + \frac{W_o}{4\pi} \sum_{\substack{j=-N \\ j \neq 0}}^{N} w_j P_S(\xi_i, \xi_j) I_{a\upsilon}(\tau, \xi_j)$$

$$+ \frac{W_o}{4\pi} P(\mu_i) e^{-\tau} \cos(\omega' \upsilon \tau) \tag{3.3.1a}$$

and

$$\mu_i \frac{d}{d\tau} I_{b\upsilon}(\tau, \xi_i) = -I_{b\upsilon}(\tau, \xi_i) + \kappa_{i\upsilon} I_{a\upsilon}(\tau, \xi_i) + \frac{W_o}{4\pi} \sum_{\substack{j=-N \\ j \neq 0}}^{N} w_j P_S(\xi_i, \xi_j) I_{b\upsilon}(\tau, \xi_j)$$

$$- \frac{W_o}{4\pi} P(\mu_i) e^{-\tau} \sin(\omega' \upsilon \tau) \quad , \tag{3.3.1b}$$

where
$$\kappa_{i\upsilon} = -\omega' \upsilon + \kappa \sqrt{1 - \mu_i^2} \, \alpha_i \tag{3.3.1c}$$

and the dependence of $\bar{I}_{a\upsilon}$ and $\bar{I}_{b\upsilon}$ on κ is suppressed.

In matrix form, (3.3.1a,b) become[**]:

$$\frac{d}{d\tau} \begin{bmatrix} \bar{I}_{a\upsilon} \\ \bar{I}_{b\upsilon} \end{bmatrix} = \begin{bmatrix} \tilde{A}_1 & \tilde{A}_2 \\ \tilde{A}_3 & \tilde{A}_4 \end{bmatrix} \begin{bmatrix} \bar{I}_{a\upsilon} \\ \bar{I}_{b\upsilon} \end{bmatrix} + \begin{bmatrix} \bar{B}_a \cos(\omega' \upsilon \tau) \\ \bar{B}_b \sin(\omega' \upsilon \tau) \end{bmatrix} e^{-\tau}, \tag{3.3.2}$$

where $\bar{I}_{a\upsilon}, \bar{I}_{b\upsilon}, \bar{B}_a, \bar{B}_b$ are column vectors of length 2N and $\tilde{A}_1, \tilde{A}_2, \tilde{A}_3, \tilde{A}_4$ are each 2N x 2N sub-matrices which are not shown here explicitly, but can easily be determined from (3.3.1a,b). It can also be shown that $\tilde{A}_1 = \tilde{A}_4$, $\tilde{A}_2 = -\tilde{A}_3$ and $\bar{B}_a = -\bar{B}_b$.

---

[*] The single index " i " is used here in place of q for convenience and is understood to represent double indices as specified in (3.2.5a).

[**] In obtaining the matrices $\tilde{A}_i$, $i = 1, \cdots, 4$, it is convenient to use the relation $\mu_{-k} = -\mu_k$, $w_{-k} = w_k$ and to write

$$\sum_{j=-N}^{N} w_j P_S(\xi_i, \xi_j) I_{x\upsilon}(\tau, \xi_j) = \sum_{k=1}^{N} [w_k P_S(\xi_i, \xi_k) I_{x\upsilon}(\tau, \xi_k) + w_{-k} P_S(\xi_i, \xi_{-k}) I_{x\upsilon}(\tau, \xi_{-k})].$$

In order to solve the above system of ordinary differential equations, the method known as variation of parameters is used [17]. The particular solution is found first and then the complementary solution. The sum of the two solutions gives the total solution to the transformed system of equations.

3.4 The Particular Solution

Expanding equation (3.3.2) by rows gives:

$$\frac{d}{d\tau}\bar{I}_{a\upsilon} = \tilde{A}_1\bar{I}_{a\upsilon} + \tilde{A}_2\bar{I}_{b\upsilon} + \bar{B}_a e^{-\tau}\cos(\omega'\upsilon\tau) \qquad (3.4.1a)$$

and

$$\frac{d}{d\tau}\bar{I}_{b\upsilon} = -\tilde{A}_2\bar{I}_{a\upsilon} + \tilde{A}_1\bar{I}_{b\upsilon} - \bar{B}_a e^{-\tau}\sin(\omega'\upsilon\tau). \qquad (3.4.1b)$$

Let $\bar{I}_{a\upsilon}$ and $\bar{I}_{b\upsilon}$ be solutions of the form:

$$\bar{I}_{a\upsilon,p} = [\bar{k}_1\cos(\omega'\upsilon\tau) + \bar{k}_2\sin(\omega'\upsilon\tau)]e^{-\tau} \qquad (3.4.2a)$$

and

$$\bar{I}_{b\upsilon,p} = [\bar{k}_3\cos(\omega'\upsilon\tau) + \bar{k}_4\sin(\omega'\upsilon\tau)]e^{-\tau}, \qquad (3.4.2b)$$

where $\bar{k}_1, \bar{k}_2, \bar{k}_3$ and $\bar{k}_4$ are each column vectors of length 2N. Substituting (3.4.2) into (3.4.1) yields the following equations:

$$-\bar{k}_1[(\omega'\upsilon)\sin(\omega'\upsilon\tau) + \cos(\omega'\upsilon\tau)]e^{-\tau} + \bar{k}_2[(\omega'\upsilon)\cos(\omega'\upsilon\tau) - \sin(\omega'\upsilon\tau)]e^{-\tau}$$
$$= \tilde{A}_1[\bar{k}_1\cos(\omega'\upsilon\tau) + \bar{k}_2\sin(\omega'\upsilon\tau)]e^{-\tau} + \tilde{A}_2[\bar{k}_3\cos(\omega'\upsilon\tau) + \bar{k}_4\sin(\omega'\upsilon\tau)]e^{-\tau}$$
$$+ \bar{B}_a e^{-\tau}\cos(\omega'\upsilon\tau)$$

$$(3.4.3a)$$

and

$$-\bar{k}_3[(\omega'\upsilon)\sin(\omega'\upsilon\tau) + \cos(\omega'\upsilon\tau)]e^{-\tau} + \bar{k}_4[(\omega'\upsilon)\cos(\omega'\upsilon\tau) - \sin(\omega'\upsilon\tau)]e^{-\tau}$$
$$= -\tilde{A}_2[\bar{k}_1\cos(\omega'\upsilon\tau) + \bar{k}_2\sin(\omega'\upsilon\tau)]e^{-\tau} + \tilde{A}_1[\bar{k}_3\cos(\omega'\upsilon\tau) + \bar{k}_4\sin(\omega'\upsilon\tau)]e^{-\tau}$$
$$- \bar{B}_a e^{-\tau}\sin(\omega'\upsilon\tau) \quad .$$

$$(3.4.3b)$$

Coefficients of the linearly independent $\cos(\omega'\upsilon\tau)$ and $\sin(\omega'\upsilon\tau)$ terms are set equal to zero to give

- $\cos(\omega'\upsilon\tau)$:
$$\begin{aligned} -\bar{k}_1 + (\omega'\upsilon)\bar{k}_2 &= \tilde{A}_1\bar{k}_1 + \tilde{A}_2\bar{k}_3 + \bar{B}_a \\ -\bar{k}_3 + (\omega'\upsilon)\bar{k}_4 &= -\tilde{A}_2\bar{k}_1 + \tilde{A}_1\bar{k}_3 \end{aligned}$$
(3.4.4a)

- $\sin(\omega'\upsilon\tau)$:
$$\begin{aligned} -(\omega'\upsilon)\bar{k}_1 - \bar{k}_2 &= \tilde{A}_1\bar{k}_2 + \tilde{A}_2\bar{k}_4 \\ -(\omega'\upsilon)\bar{k}_3 - \bar{k}_4 &= -\tilde{A}_2\bar{k}_2 + \tilde{A}_1\bar{k}_4 - \bar{B}_a \end{aligned}$$
(3.4.4b)

Re-writing equation (3.4.4a-b) in matrix form yields:

$$\begin{bmatrix} \tilde{A}_1 + \tilde{I}_{2N} & -(\omega'\upsilon)\tilde{I}_{2N} & \tilde{A}_2 & \tilde{0} \\ +(\omega'\upsilon)\tilde{I}_{2N} & \tilde{A}_1 + \tilde{I}_{2N} & \tilde{0} & \tilde{A}_2 \\ -\tilde{A}_2 & \tilde{0} & \tilde{A}_1 + \tilde{I}_{2N} & -(\omega'\upsilon)\tilde{I}_{2N} \\ \tilde{0} & -\tilde{A}_2 & +(\omega'\upsilon)\tilde{I}_{2N} & \tilde{A}_1 + \tilde{I}_{2N} \end{bmatrix} \begin{bmatrix} \bar{k}_1 \\ \bar{k}_2 \\ \bar{k}_3 \\ \bar{k}_4 \end{bmatrix} = - \begin{bmatrix} \bar{B}_a \\ \bar{0} \\ \bar{0} \\ -\bar{B}_a \end{bmatrix} ,$$
(3.4.5)

where
$$\bar{B}_a = \begin{bmatrix} b_1 \\ \vdots \\ b_2 \\ b_{-1} \\ \vdots \\ b_{-N} \end{bmatrix} .$$
(3.4.6)

$\tilde{I}_{2N}$ is the identity matrix of size $2N \times 2N$ and $\bar{0}$ is the zero column vector of length 2N. Equation (3.4.5) is written in compact form as

$$[\tilde{A}_\upsilon + \tilde{I}_{8N}]\bar{K}_\upsilon = -\bar{B}_\upsilon \quad ,$$
(3.4.7)

where $\tilde{A}_\upsilon$ is an $8N \times 8N$ square matrix, $\bar{K}_\upsilon$ and $\bar{B}_\upsilon$ are column vectors of length 8N, and $\tilde{I}_{8N}$ is the $8N \times 8N$ identity matrix. From (3.4.7), the $\bar{K}_\upsilon$ vector is found to be

$$\bar{K}_\upsilon = -[\tilde{A}_\upsilon + \tilde{I}_{8N}]^{-1}\bar{B}_\upsilon \quad ,$$
(3.4.8)

where the $\widetilde{A}_\upsilon$ matrix is given by

$$\widetilde{A}_\upsilon = \begin{bmatrix} \widetilde{A}_1 & -(\omega'\upsilon)\widetilde{I}_{2N} & \widetilde{A}_2 & \widetilde{0} \\ +(\omega'\upsilon)\widetilde{I}_{2N} & \widetilde{A}_1 & \widetilde{0} & \widetilde{A}_2 \\ -\widetilde{A}_2 & \widetilde{0} & \widetilde{A}_1 & -(\omega'\upsilon)\widetilde{I}_{2N} \\ \widetilde{0} & -\widetilde{A}_2 & +(\omega'\upsilon)\widetilde{I}_{2N} & \widetilde{A}_1 \end{bmatrix}. \qquad (3.4.9)$$

With the $\overline{K}_\upsilon$ vector known from (3.4.8), the particular solution (3.4.2) takes the form:

$$\overline{I}_{p\upsilon} = \begin{bmatrix} \overline{I}_{a\upsilon.p} \\ \overline{I}_{b\upsilon,p} \end{bmatrix} = \begin{bmatrix} \overline{k}_1 & \overline{k}_2 \\ \overline{k}_3 & \overline{k}_4 \end{bmatrix} \times \begin{bmatrix} \cos(\omega'\upsilon\tau) \\ \sin(\omega'\upsilon\tau) \end{bmatrix} e^{-\tau}. \qquad (3.4.10)$$

To compare the above result to that of Chang and Ishimaru [12], the parameter υ is set to zero in (3.4.5), which yields

$$\begin{bmatrix} \widetilde{A}_1 + \widetilde{I}_{2N} & \widetilde{0} & \widetilde{A}_2 & \widetilde{0} \\ \widetilde{0} & \widetilde{A}_1 + \widetilde{I}_{2N} & \widetilde{0} & \widetilde{A}_2 \\ -\widetilde{A}_2 & \widetilde{0} & \widetilde{A}_1 + \widetilde{I}_{2N} & \widetilde{0} \\ \widetilde{0} & -\widetilde{A}_2 & \widetilde{0} & \widetilde{A}_1 + \widetilde{I}_{2N} \end{bmatrix} \begin{bmatrix} \overline{k}_1 \\ \overline{k}_2 \\ \overline{k}_3 \\ \overline{k}_4 \end{bmatrix} = - \begin{bmatrix} \overline{B}_a \\ \overline{0} \\ \overline{0} \\ -\overline{B}_a \end{bmatrix}. \qquad (3.4.11)$$

The equations in (3.4.11) decouple and separate into the two smaller systems of equations given in (3.4.12) and (3.4.14) below. Consider the former one,

$$\begin{bmatrix} \widetilde{A}_1 + \widetilde{I}_{2N} & \widetilde{A}_2 \\ -\widetilde{A}_2 & \widetilde{A}_1 + \widetilde{I}_{2N} \end{bmatrix} \begin{bmatrix} \overline{k}_1 \\ \overline{k}_3 \end{bmatrix} = - \begin{bmatrix} \overline{B}_a \\ \overline{0} \end{bmatrix}. \qquad (3.4.12)$$

Solving for $\bar{k}_1$ and $\bar{k}_3$ gives

$$\begin{bmatrix} \bar{k}_1 \\ \bar{k}_3 \end{bmatrix} = -[\tilde{A}_o + \tilde{I}_{4N}]^{-1} \bar{B}' , \tag{3.4.13}$$

where

$$\tilde{A}_o = \begin{bmatrix} \tilde{A}_1 & \tilde{A}_2 \\ -\tilde{A}_2 & \tilde{A}_1 \end{bmatrix} \quad , \quad \bar{B}' = \begin{bmatrix} \bar{B}_a \\ \bar{0} \end{bmatrix} \tag{3.4.13a}$$

and $\tilde{I}_{4N}$ is the identity matrix of size 4N x 4N. The second smaller system

$$\begin{bmatrix} \tilde{A}_1 + \tilde{I}_{2N} & \tilde{A}_2 \\ -\tilde{A}_2 & \tilde{A}_1 + \tilde{I}_{2N} \end{bmatrix} \begin{bmatrix} \bar{k}_2 \\ \bar{k}_4 \end{bmatrix} = -\begin{bmatrix} \bar{0} \\ -\bar{B}_a \end{bmatrix} \tag{3.4.14}$$

yields

$$\begin{bmatrix} \bar{k}_2 \\ \bar{k}_4 \end{bmatrix} = -[\tilde{A}_o + \tilde{I}_{4N}]^{-1} \bar{B}'' , \tag{3.4.15}$$

where

$$\bar{B}'' = \begin{bmatrix} \bar{0} \\ -\bar{B}_a \end{bmatrix} . \tag{3.4.15a}$$

Hence for the $\upsilon = 0$ case, (3.4.10) takes the form:

$$\bar{I}_{p0} = \begin{bmatrix} \bar{k}_1 & \bar{k}_2 \\ \bar{k}_3 & \bar{k}_4 \end{bmatrix} \begin{bmatrix} 1 \\ 0 \end{bmatrix} e^{-\tau} = \begin{bmatrix} \bar{k}_1 \\ \bar{k}_3 \end{bmatrix} e^{-\tau} = -[\tilde{A}_o + \tilde{I}_{4N}]^{-1} \begin{bmatrix} \bar{B}_a \\ 0 \end{bmatrix} e^{-\tau} . \tag{3.4.16}$$

Observe that the particular solution (3.4.16) agrees with Chang and Ishimaru [12] which corresponds to the time-independent case ($\upsilon = 0$).

3.5 The Complementary Solution

The homogeneous system of differential equation for the time-dependent bounded beam problem, i.e., (3.3.2) with $\overline{B}_a = \overline{0}$, has the same form as found in [12] for the time-independent bounded beam problem. Therefore, the system is solved by using the method developed by Chang and Ishimaru. The complementary solution is found by solving the homogeneous system of differential equations in (3.3.2), which is written in expanded form as

$$
\frac{d}{d\tau}
\begin{bmatrix}
\overline{I}_{a\upsilon}^+ \\[6pt]
\overline{I}_{a\upsilon}^- \\[6pt]
\overline{I}_{b\upsilon}^+ \\[6pt]
\overline{I}_{b\upsilon}^-
\end{bmatrix}
=
\begin{bmatrix}
+\tilde{A}_1^\upsilon & +\tilde{A}_2^\upsilon & +\tilde{K}^\upsilon & \tilde{0} \\[6pt]
-\tilde{A}_2^\upsilon & -\tilde{A}_1^\upsilon & \tilde{0} & -\tilde{K}^\upsilon \\[6pt]
-\tilde{K}^\upsilon & \tilde{0} & +\tilde{A}_1^\upsilon & +\tilde{A}_2^\upsilon \\[6pt]
\tilde{0} & +\tilde{K}^\upsilon & -\tilde{A}_2^\upsilon & -\tilde{A}_1^\upsilon
\end{bmatrix}
\begin{bmatrix}
\overline{I}_{a\upsilon}^+ \\[6pt]
\overline{I}_{a\upsilon}^- \\[6pt]
\overline{I}_{b\upsilon}^+ \\[6pt]
\overline{I}_{b\upsilon}^-
\end{bmatrix}
, \qquad (3.5.1)
$$

where the N x N real matrices $\tilde{A}_1^\upsilon$ and $\tilde{A}_2^\upsilon$ may be obtained by comparison with (3.3.1a,b) and $\tilde{K}^\upsilon$ is an N x N diagonal real matrix.

The above system is rearranged to demonstrate the coupling between the forward $(0 < \mu < 1)$ and the backward $(-1 < \mu < 0)$ specific intensities. Therefore, the order of the specific intensity vector is modified as follow

$$
\overline{I}_{c\upsilon}(\tau) =
\begin{bmatrix}
\overline{I}_{a\upsilon}^+ \\[6pt]
\overline{I}_{b\upsilon}^+ \\[6pt]
\overline{I}_{a\upsilon}^- \\[6pt]
\overline{I}_{b\upsilon}^-
\end{bmatrix}
, \qquad
\overline{I}_{x\upsilon}^{\pm}(\tau) =
\begin{bmatrix}
\overline{I}_{x\upsilon}(\tau,\xi_{\pm 1}) \\[6pt]
\overline{I}_{x\upsilon}(\tau,\xi_{\pm 2}) \\[6pt]
\vdots \\[6pt]
\overline{I}_{x\upsilon}(\tau,\xi_{\pm N})
\end{bmatrix}
, x = a,b \quad . \qquad (3.5.2)
$$

Note that the dependence on κ is suppressed. The new system of differential equations are obtained by interchanging row 2 and row 3, while keeping in mind that each element of the resulting matrix is an N x N matrix. Hence,

$$\frac{d}{d\tau}\begin{bmatrix} \bar{I}_{a\upsilon}^{+} \\ \bar{I}_{b\upsilon}^{+} \\ \bar{I}_{a\upsilon}^{-} \\ \bar{I}_{b\upsilon}^{-} \end{bmatrix} = \begin{bmatrix} +\widetilde{A}_{1}^{\upsilon} & +\widetilde{K}^{\upsilon} & +\widetilde{A}_{2}^{\upsilon} & \widetilde{0} \\ -\widetilde{K}^{\upsilon} & +\widetilde{A}_{1}^{\upsilon} & \widetilde{0} & +\widetilde{A}_{2}^{\upsilon} \\ -\widetilde{A}_{2}^{\upsilon} & \widetilde{0} & -\widetilde{A}_{1}^{\upsilon} & -\widetilde{K}^{\upsilon} \\ \widetilde{0} & -\widetilde{A}_{2}^{\upsilon} & +\widetilde{K}^{\upsilon} & -\widetilde{A}_{1}^{\upsilon} \end{bmatrix}\begin{bmatrix} \bar{I}_{a\upsilon}^{+} \\ \bar{I}_{b\upsilon}^{+} \\ \bar{I}_{a\upsilon}^{-} \\ \bar{I}_{b\upsilon}^{-} \end{bmatrix} . \qquad (3.5.3)$$

The 4N × 4N system of differential equations in (3.5.3) is rewritten in terms of an anti-symmetric matrix:

$$\frac{d}{d\tau}\begin{bmatrix} \bar{I}_{c\upsilon}^{+}(\tau) \\ \bar{I}_{c\upsilon}^{-}(\tau) \end{bmatrix} = \begin{bmatrix} -\widetilde{A}_{1\upsilon} & -\widetilde{A}_{2\upsilon} \\ \widetilde{A}_{2\upsilon} & \widetilde{A}_{1\upsilon} \end{bmatrix}\begin{bmatrix} \bar{I}_{c\upsilon}^{+}(\tau) \\ \bar{I}_{c\upsilon}^{-}(\tau) \end{bmatrix} \qquad (3.5.4a)$$

or succinctly as

$$\frac{d}{d\tau}\bar{I}_{c\upsilon}(\tau) = \widetilde{A}_{c\upsilon}\bar{I}_{c\upsilon} \quad , \qquad (3.5.4b)$$

where $\widetilde{A}_{1\upsilon}$ and $\widetilde{A}_{2\upsilon}$ are 2N × 2N matrices. Using (3.5.2), the 2N-column vector $\bar{I}_{c\upsilon}^{\pm}(\tau)$ is given by

$$\bar{I}_{c\upsilon}^{\pm}(\tau) = \begin{bmatrix} I_{a\upsilon}(\tau,\xi_{\pm 1}) \\ \vdots \\ I_{a\upsilon}(\tau,\xi_{\pm N}) \\ I_{b\upsilon}(\tau,\xi_{\pm 1}) \\ \vdots \\ I_{b\upsilon}(\tau,\xi_{\pm N}) \end{bmatrix} . \qquad (3.5.5)$$

The solution to the homogeneous equation (3.5.4) takes the form [1, 12]:

$$\bar{I}_{c\upsilon}(\tau) = \overline{\beta}e^{\lambda\tau} \quad , \qquad (3.5.6)$$

where λ and $\overline{\beta}$ are, respectively, the eigenvalues and the correspondence eigenvectors of the matrix in (3.5.3) or (3.5.4). Denote the eigenvalues as $\lambda_{\pm n}$ and the associated eigenvectors as

$$\bar{\beta}_{\pm n} = \begin{bmatrix} \beta_{1,\pm n} \\ \vdots \\ \beta_{2N,\pm n} \\ \beta_{-1,\pm n} \\ \vdots \\ \beta_{-2N,\pm n} \end{bmatrix} \quad , \quad n = 1,2,\cdots,2N \quad . \tag{3.5.7}$$

Because of the anti-symmetric nature of $\tilde{A}_{c\upsilon}$, the eigenvalues and eigenvectors obey the relationships [1, 12]

$$\lambda_n = -\lambda_{-n} \qquad \text{and} \qquad \beta_{i,n} = \beta_{-i,-n} \quad . \tag{3.5.8}$$

The eigenvectors with a positive index represent propagation and attenuation in the forward direction. Therefore, the real part of the associated eigenvalues must be negative. Similarly, the eigenvectors with a negative index represent propagation and attenuation in the backward direction and the real part of the associated eigenvalues must be positive. As a result, the complementary solution is expressed as a linear combination of all the eigervectors with different expansion coefficients. The solution takes the form

$$\bar{I}_{c\upsilon}(\tau) = \sum_{n=1}^{2N} c_n \bar{\beta}_n e^{\lambda_n \tau} + \sum_{n=1}^{2N} c_{-n} \bar{\beta}_{-n} e^{\lambda_{-n}(\tau-\tau_o)} \tag{3.5.9}$$

with $Re(\lambda_n) < 0 \quad and \quad Re(\lambda_{-n}) > 0$ or by use of equation (3.5.8) as

$$\bar{I}_{c\upsilon}(\tau) = \sum_{n=1}^{2N} c_n \bar{\beta}_n e^{-\lambda_{-n}\tau} + \sum_{n=1}^{2N} c_{-n} \bar{\beta}_{-n} e^{-\lambda_{-n}(\tau_o-\tau)} \quad . \tag{3.5.10}$$

It can be expressed in the matrix form

$$\bar{I}_{c\upsilon}(\tau) = \begin{bmatrix} \tilde{U}_1 e^{-\tilde{\Lambda}\tau} \bar{C}^+ & + & \tilde{U}_2 e^{-\tilde{\Lambda}(\tau_o-\tau)} \bar{C}^- \\ \tilde{U}_3 e^{-\tilde{\Lambda}\tau} \bar{C}^+ & + & \tilde{U}_4 e^{-\tilde{\Lambda}(\tau_o-\tau)} \bar{C}^- \end{bmatrix} \quad , \tag{3.5.11}$$

where $e^{-\tilde{\Lambda}\tau}$ is a 2N × 2N diagonal matrix of the form

$$e^{-\tilde{\Lambda}\tau} \equiv \begin{bmatrix} e^{-\lambda_1\tau} & & 0 \\ & \ddots & \\ 0 & & e^{-\lambda_{2N}\tau} \end{bmatrix} \tag{3.5.11a}$$

and
$$\tilde{U}_1 = \begin{bmatrix} \beta_{1,1} & \cdots & \beta_{2N,1} \\ \beta_{1,2} & \cdots & \beta_{2N,2} \\ \vdots & \cdots & \vdots \\ \beta_{1,2N} & \cdots & \beta_{2N,2N} \end{bmatrix} \; , \; \tilde{U}_2 = \begin{bmatrix} \beta_{-1,1} & \cdots & \beta_{-2N,1} \\ \beta_{-1,2} & \cdots & \beta_{-2N,2} \\ \vdots & \cdots & \vdots \\ \beta_{-1,2N} & \cdots & \beta_{-2N,2N} \end{bmatrix} \; , \tag{3.5.11b}$$

$$\tilde{U}_3 = \begin{bmatrix} \beta_{1,-1} & \cdots & \beta_{2N,-1} \\ \beta_{1,-2} & \cdots & \beta_{2N,-2} \\ \vdots & \cdots & \vdots \\ \beta_{1,-2N} & \cdots & \beta_{2N,-2N} \end{bmatrix} \; , \; \tilde{U}_4 = \begin{bmatrix} \beta_{-1,-1} & \cdots & \beta_{-2N,-1} \\ \beta_{-1,-2} & \cdots & \beta_{-2N,-2} \\ \vdots & \cdots & \vdots \\ \beta_{-1,-2N} & \cdots & \beta_{-2N,-2N} \end{bmatrix} \; . \tag{3.5.11c}$$

In order to combine the particular and complementary solutions, (3.5.10) is written in matrix notation as

$$\overline{I}_{cv} = \begin{bmatrix} \overline{I}_{cv}^+(\tau) \\ \overline{I}_{cv}^-(\tau) \end{bmatrix} = \begin{bmatrix} \tilde{U}_1 & \tilde{U}_2 \\ \tilde{U}_3 & \tilde{U}_4 \end{bmatrix} \begin{bmatrix} e^{-\tilde{\Lambda}\tau} & \tilde{0} \\ \tilde{0} & e^{-\tilde{\Lambda}(\tau_o-\tau)} \end{bmatrix} \begin{bmatrix} \overline{C}^+ \\ \overline{C}^- \end{bmatrix} \; . \tag{3.5.12}$$

$\overline{C}^\pm$ are column vectors of length 2N whose entities consist of

$$\overline{C} \equiv \begin{bmatrix} \overline{C}^+ \\ \overline{C}^- \end{bmatrix} = \begin{bmatrix} c_1 \\ \vdots \\ c_{2N} \\ c_{-1} \\ \vdots \\ c_{-2N} \end{bmatrix} \tag{3.5.13a}$$

and
$$\tilde{U} = \begin{bmatrix} \tilde{U}_1 & \tilde{U}_2 \\ \tilde{U}_3 & \tilde{U}_4 \end{bmatrix} = [\overline{\beta}_1, \overline{\beta}_2, \cdots\cdots, \overline{\beta}_{2N}, \overline{\beta}_{-1}, \overline{\beta}_{-2} \cdots\cdots, \overline{\beta}_{-2N}] \tag{3.5.13b}$$

with $\beta_{\pm n}$, $n=1, 2\cdots$, $2N$ given in (3.5.7).

3.6 The Total Solution

In order to add the particular and complementary solutions together, the particular solution in (3.4.10) must be written in the same form as the complementary solution. Hence,

$$
\bar{I}_{p\upsilon}(\tau) = \begin{bmatrix} \bar{I}_{a\upsilon}^+ \\ \bar{I}_{b\upsilon}^+ \\ \bar{I}_{a\upsilon}^- \\ \bar{I}_{b\upsilon}^- \end{bmatrix} = \begin{bmatrix} \bar{k}_1^+ & \bar{k}_2^+ \\ \bar{k}_3^+ & \bar{k}_4^+ \\ \bar{k}_1^- & \bar{k}_2^- \\ \bar{k}_3^- & \bar{k}_4^- \end{bmatrix} \begin{bmatrix} e^{-\tau}\cos(\omega'\upsilon\tau) \\ \\ e^{-\tau}\sin(\omega'\upsilon\tau) \end{bmatrix} \, . \tag{3.6.1}
$$

Therefore, the total diffuse intensity solution to the time-dependent beam wave problem in transform space (κ, ψ_κ) in matrix notation takes the form:

$$
\bar{I}_{T\upsilon}(\tau) = \begin{bmatrix} \tilde{U}_1 & \tilde{U}_2 \\ \\ \tilde{U}_3 & \tilde{U}_4 \end{bmatrix} \begin{bmatrix} e^{-\tilde{\Lambda}\tau} & \tilde{0} \\ \\ \tilde{0} & e^{-\tilde{\Lambda}(\tau_o-\tau)} \end{bmatrix} \begin{bmatrix} \bar{C}^+ \\ \\ \bar{C}^- \end{bmatrix} + \begin{bmatrix} \bar{k}_1^+ & \bar{k}_2^+ \\ \bar{k}_3^+ & \bar{k}_4^+ \\ \bar{k}_1^- & \bar{k}_2^- \\ \bar{k}_3^- & \bar{k}_4^- \end{bmatrix} \begin{bmatrix} e^{-\tau}\cos(\omega'\upsilon\tau) \\ \\ e^{-\tau}\sin(\omega'\upsilon\tau) \end{bmatrix} \, .
$$

$$\tag{3.6.2}$$

For convenience, $\bar{I}_{T\upsilon}$ is written showing only its dependence on τ, but in reality it depends on the four variables $(\tau, \kappa, \mu, \psi_\kappa)$.

Recall from (3.1.11) that $I_{F,x\upsilon} = S_p f_\upsilon A_w e^{-\kappa^2/\kappa_o^2} I_{x\upsilon}$, where $x=a,\ b$ and also from (3.1.4) that $I_{F\upsilon}(\tau,\kappa,\mu,\psi_\kappa) = I_{F,a\upsilon}(\tau,\kappa,\mu,\psi_\kappa) + i I_{F,b\upsilon}(\tau,\kappa,\mu,\psi_\kappa)$ is the Fourier-Bessel transform of the diffuse intensity $I_{d\upsilon}(\tau,\tau_\rho,\mu,\psi)$; see (2.3.5). To determine the constant $\bar{C}$ vector in (3.5.13a) and (3.6.2), the boundary conditions in (3.1.1a) expressed as[*]

$$
\bar{I}_{F\upsilon}^+(\tau=0) = \bar{0} \quad \text{and} \quad \bar{I}_{F\upsilon}^-(\tau=\tau_o) = \bar{0} \tag{3.6.3}
$$

are used to obtain the following linear system of equations

---

[*] The " + " superscript designates intensity flow in the forward direction $(0 \le \mu \le 1)$ while the " - " superscript designates intensity flow in the backward direction $(-1 \le \mu \le 0)$.

$$
\begin{bmatrix} \tilde{U}_1 & \tilde{U}_2 e^{-\tilde{\Lambda}\tau_o} \\ \tilde{U}_3 e^{-\tilde{\Lambda}\tau_o} & \tilde{U}_4 \end{bmatrix} \begin{bmatrix} \overline{C}^+ \\ \overline{C}^- \end{bmatrix} = - \begin{bmatrix} \overline{k}_1^+ \\ \overline{k}_3^+ \\ \begin{bmatrix} \overline{k}_1^- & \overline{k}_2^- \\ \overline{k}_3^- & \overline{k}_4^- \end{bmatrix} \begin{bmatrix} e^{-\tau_o} \cos(\omega'\upsilon\tau_o) \\ e^{-\tau_o} \sin(\omega'\upsilon\tau_o) \end{bmatrix} \end{bmatrix} .
\tag{3.6.4}
$$

Equation (3.6.4) is numerically stable in the sense that as $\tau_o \to \infty$, $\overline{C}^- = \overline{0}$ which was expected for the semi-infinite medium.

Equation (3.6.2) constitutes the complete diffuse intensity solution in the Fourier-Bessel transform domain for a bounded beam that is incident on a slab of optical thickness τ_o. To obtain the solution in the space domain, the inverse Fourier-Bessel transform of equation (3.6.2) is taken using (2.3.5b) with (3.1.4) and (3.1.11) to give[*]

$$
I_{d\upsilon}(\tau, \tau_\rho, \mu, \psi) = \frac{\sigma_t^2}{(2\pi)^2} \int\limits_0^\infty \int\limits_0^{2\pi} S_p f_\upsilon A_w e^{-\kappa^2/\kappa_o^2} [I_{a\upsilon} + i I_{b\upsilon}] e^{-i\kappa\tau_\rho \cos(\psi-\psi_\kappa)} d\psi_\kappa \kappa \, d\kappa
$$

$$
\tag{3.6.5}
$$

and the result added to the reduced incident specific intensity in (2.2.8). In the next chapter, the scattering and propagation of beam pulses incident on a half space $(\tau_o \to \infty)$ are found for which numerical results are obtained.

---

[*] Note in (3.6.5) that $\sigma_t^2 A_w = \pi(\sigma_t w)^2 = \pi \, w'^2 \equiv A_{w'}$. Thus, $I_{d\upsilon}$ depends on w' via $A_{w'}$ and $\kappa_o = 2/w'$. In numerical evaluation, therefore, w' needs to be specified, not w and σ_t separately.

CHAPTER 4

PULSE BEAM WAVE PROPAGATION IN A SEMI-FINITE MEDIUM

In the previous chapter, a theory to study the scattering and propagation of a pulse beam-wave train incident on a slab of fixed optical thickness using the scalar time-dependent transport equation was presented. In this chapter, the theory is used to study the propagation of beam-wave pulses incident on a semi-infinite medium.

4.1 Gaussian Beam-wave Pulses

The medium is assumed to occupy the half-space region $z \geq 0$ (see Figure 1). A beam-wave pulse train from the air region $z < 0$ is assumed to be normally incident onto the medium. At $z = 0$, the magnitude of the instantaneous Poynting vector of the incident signal is expressed as

$$S(0,\rho,t) = S_p A(\rho) f(0,t) \cos(\omega_c t) \quad , \tag{4.1.1}$$

where ω_c is the angular carrier frequency, $f(0,\rho,t)$ is an even function of time t normalized such that at $z = 0$, $\rho = 0$

$$\frac{1}{T} \int_{-T/2}^{T/2} f(0,t) dt = 1 \tag{4.1.2}$$

and S_p is the time-averaged Poynting vector at the origin; T is the pulse repetition rate.

The shape of the incident beam pulse is arbitrary. For simplicity, assume normalized Gaussian incident beam-wave pulses that at $z = 0$ and $\rho = 0$ are given by

$$f(0,t) = \frac{\alpha_0}{\sqrt{\pi}} e^{-(\alpha_0 t/T)^2} \quad , \quad -\frac{T}{2} \leq t \leq \frac{T}{2} \quad . \tag{4.1.3}$$
$$\alpha_0 \equiv const.$$

Since the incident beam-wave pulses are even, periodic functions of time, they can be represented by the even Fourier series at $z = 0$:

$$f(0,t) = [\frac{b_o}{2} + \sum_{\upsilon=1}^{\infty} b_\upsilon \cos(\upsilon \omega t)] = \text{Re}\{\sum_{\upsilon=0}^{\infty} f_\upsilon e^{i\upsilon \omega t}\} \quad , \tag{4.1.4}$$

where

$$\omega = \frac{2\pi}{T} \quad , \quad b_\upsilon = \frac{2}{T} \int\limits_{-T/2}^{T/2} f(0,t)\cos(\upsilon\omega t)dt \quad .$$
(4.1.5)

Hence, for the Gaussian beam-wave pulse train

$$f_\upsilon = \frac{\varepsilon_\upsilon b_\upsilon}{2} = \varepsilon_\upsilon e^{-(\pi\upsilon/\alpha_o)^2} \quad , \quad \varepsilon_\upsilon = \begin{Bmatrix} 1, & \upsilon = 0 \\ 2, & \upsilon \neq 0 \end{Bmatrix} \quad .$$
(4.1.6)

α_o has to be chosen properly to insure that the Gaussian function in equation (4.1.3) goes to zero at $t \to \pm\dfrac{T}{2}$.

In Chapter 2, the reduced incident intensity is given in (2.2.8). Substituting (4.1.6) into (2.2.8) yields:

$$I_{ri,\upsilon}(z,\rho,\theta) = S_p \varepsilon_\upsilon e^{-(\pi\upsilon/\alpha_o)^2}\, e^{-(\rho^2/w^2)} e^{-\eta_\upsilon \tau} \frac{\delta(\theta)}{2\pi\sin(\theta)} \quad .$$
(4.1.7)

The diffuse intensity is found by following the procedure developed in Chapter 3; see (3.6.5). The specific intensity is calculated only along the beam center axis ($\rho=0$) because solutions off the beam center involves Bessel functions and would require more computer resources. The transformed source function of the infinite half–space is expressed as (see (2.4.6))

$$E_\upsilon(\tau,\kappa,\mu) = \frac{W_o}{4\pi} S_p (\pi w^2) \varepsilon_\upsilon e^{-(\pi\upsilon/\alpha_o)^2} e^{-\eta_\upsilon \tau} P(\mu) e^{-\kappa^2/\kappa_o^2} \quad .$$
(4.1.8)

4.2 The Semi-Infinite Medium (special case)

As mentioned in Chapter 3, as $\tau_o \to \infty$ the backscattered part of the complementary solution vanishes, namely, $\overline{C}^- = 0$. This result and the value of the $\overline{C}^+$ vector are obtained by direct substitution of $\tau_o \to \infty$ into (3.6.4), recalling that $\mathrm{Re}(\lambda_{-n}) > 0$, to yield

$$\begin{bmatrix} \overline{0} \\ \overline{0} \end{bmatrix} = \begin{bmatrix} \widetilde{U}_1 & \widetilde{0} \\ \widetilde{0} & \widetilde{U}_4 \end{bmatrix} \begin{bmatrix} \overline{C}^+ \\ \overline{C}^- \end{bmatrix} + \begin{bmatrix} \overline{k}_1^+ \\ \overline{k}_3^+ \\ \overline{0} \\ \overline{0} \end{bmatrix} \qquad (4.2.1)$$

From (4.2.1), $\overline{C}^- = 0$ and $\overline{C}^+$ is obtained by solving the linear system

$$\widetilde{U}_1 \overline{C}^+ = -\begin{bmatrix} \overline{k}_1^+ \\ \overline{k}_3^+ \end{bmatrix} \qquad (4.2.2)$$

As a result, from (3.6.2) the Fourier-Bessel transform of the diffuse intensity in a semi-infinite media due to incident beam wave pulses incident on a semi-infinite medium takes the form:

$$\begin{aligned} \overline{I}_{Tv}(\tau) &= \overline{I}_{cv}(\tau) + \overline{I}_{pv}(\tau) \\ &= \begin{bmatrix} \widetilde{U}_1 e^{-\widetilde{\Lambda}\tau} \overline{C}^+ \\ \widetilde{U}_3 e^{-\widetilde{\Lambda}\tau} \overline{C}^+ \end{bmatrix} + \begin{bmatrix} \overline{k}_1^+ & \overline{k}_2^+ \\ \overline{k}_3^+ & \overline{k}_4^+ \\ \overline{k}_1^- & \overline{k}_2^- \\ \overline{k}_3^- & \overline{k}_4^- \end{bmatrix} \begin{bmatrix} e^{-\tau}\cos(\omega' v \tau) \\ e^{-\tau}\sin(\omega' v \tau) \end{bmatrix} \end{aligned} \qquad (4.2.3)$$

The inverse Fourier transform of (4.2.3) gives the diffuse intensity at any point in the forest. Adding this result to the inverse Fourier transform of the reduced incident intensity in (4.1.7) gives the total intensity for Gaussian beam wave pulses incident on a semi-infinite medium.

In the forest, the power is received by a highly directive antenna. For such an antenna the diffuse received power is directly proportional to the diffuse intensity. The complete derivation of the power received by such a antenna was developed in [11] and is presented in Appendix B for reference. In summary, the total power received by a highly directive antenna place in the forest is given by

$$P'(\tau, \tau_\rho, t', \theta_M, \phi_M) = P'_{ri} + P'_d \quad , \qquad (4.2.4)$$

where P'_{ri} and P'_d are the normalized reduced incident and diffuse received powers, respectively. For an antenna whose main beam direction lies in the xz-plane ($\phi_M = 0$) and is located at a normalized penetration depth τ on the beam center ($\tau_\rho = 0$) as in Figure 1, the normalized total received power is obtained from the expression

$$P'(\tau,\tau_\rho = 0, t', \theta_M, \phi_M = 0) = \mathrm{Re}\{\sum_{\upsilon=0}^{\infty} P'_\upsilon(\tau,\tau_\rho = 0, \theta_M, \phi_M = 0)e^{i\upsilon\omega' t'}\}, \qquad (4.2.5)$$

where

$$P'_\upsilon(\tau,\tau_\rho = 0, \theta_M, \phi_M = 0) = \frac{D(\theta_M)}{D(0)} f_\upsilon e^{-\eta_\upsilon \tau} + \frac{4\pi}{S_p D(0)} I_{d\upsilon}(\tau,\tau_\rho = 0, \theta_M, \phi_M = 0).$$

$$(4.2.5a)$$

The proof of (4.2.5) is given in Appendix B.

The first term in (4.2.5) reduced to

$$P'_{ri}(\tau,\tau_\rho = 0, \theta_M, \phi_M = 0) = \frac{D(\theta_M)}{D(0)} f_\upsilon e^{-\tau} f(t-\tau), \qquad (4.2.6)$$

where $\tau = \sigma_t z$ and $t' = \sigma_t ct$. This result was expected since the reduced incident intensity, as the name implies, is the power of the incident pulse train which, while traveling along a straight path into the forest, is attenuation exponentially due to the absorption and scattering (recall $\sigma_t = \sigma_A + \sigma_S$), but maintain its narrow (δ-function) beamwidth. The θ-dependence of P'_{ri} thus reproduces the radiation pattern of the receive antenna. In contrast, the diffuse intensity, generated by scattering of the reduced incident intensity and continuously regenerated by mutiple scattering, exhibits a broad beamwith substantially exceeding that of the receive antenna. Hence, when scanned, the antenna in effect " probes " the angular distribution of I_d, as indicated in (4.2.5)

In the next chapter, the numerical results are presented and comparisons are made to the data presented in [11].

CHAPTER 5

NUMERICAL RESULT

All computations are performed using several normalized parameters and normalized variables. This permits the specification of the scatter medium by the three parameters: W_o, $\Delta \gamma_s$ and α, where $W_o = \sigma_S / \sigma_t$ is the albedo and $\sigma_t = \sigma_A + \sigma_S$ is the extinction cross-section. The normalized space and time variables include: $\tau = \sigma_t z$, $\tau_\rho = \sigma_t \rho$ and $t' = \sigma_t c t$. Additional normalized parameters are: $T' = \sigma_t c T$, $\omega' = 2\pi / T' = \omega / \sigma_t c$ and $w' = \sigma_t w$.

The incident Gaussian pulses, given either by the expression in (4.1.3) or by the Fourier series representation in (4.1.4) and (4.1.5), are specified with the parameter α_0 set equal to $4\sqrt{5}$; this insures that the Gaussian pulse at $t' = \pm T'/4$ falls to $1/e^5$ times its maximum value $f(0, 0)$ given in (4.1.3). The normalized pulse repetition period T' of the incident pulse train is chosen to be 2. The truncated series representation for $\upsilon_{\max} > 12$ were found to yield values, which overlap indistinguishably from the exact values. According to (4.2.5) and (4.2.6) (also see B.17), the normalized received power P' equals $f(0, t')$ in the "reference case" for which the antenna is placed at the origin in the boundary plane $\tau = 0$, $\tau_\rho = 0$ and aligned with the incoming pulse train ($\theta_M = 0°$, $\phi_M = 0°$). Hence, the received power inside the forest at points $\tau \neq 0$ can be compared to the plot of $f(0, t')$ in Figure 6. Results of a test series conducted with CW signals [9.10] indicate that the extinction cross-section $\sigma_t = \sigma_A + \sigma_S$ in the canopy region of a modestly dense forest (orchard) is in the order of $0.1\text{-}0.5\,m^{-1}$ in the 30-60 GHz band. With σ_t in this order, the assumed value of $T' = 2$ would correspond to a pulse

repetition rate of about 5×10^7 Pulses/sec, and the pulse repetition period of 20ns would extend over 1000 cycles of a $50\,GHz$ carrier signal. These values appear reasonable for the millimeter-wave region. Under the same conditions, a normalized distance of $\tau = 1$ corresponds to a vegetation path length of 2-10m. In all subsequent cases, $W_o = 0.75$.

In Figure 2, the Gaussian scatter function is plotted using both the exact expression in (1.1) and the Legendre polynomial expansion in (17) of [11], truncated at $N = 50$, and were found to be in distinguishable. They exhibited the expected shape of a pronounced forward lobe superimposed on an isotropic background.

Using (4.2.5), the received power in the forest is computed for the antenna oriented such that its pointing direction is chosen for $\phi_M = 0°$ and for values of θ_M that were pre-determined by the Gauss quadrature formula. For a discussion of the figures to follow, it is helpful to recall some results of the corresponding CW theory [6, 7]. The reduced incident intensity dominates at small depths into the random medium ($\tau < 1$). While its beamwidth remains narrow and does not change with path length, its amplitude decreases exponentially at a relatively high attenuation rate equal to the extinction cross section of the medium $\sigma_t = \sigma_A + \sigma_S$. Both absorption and scattering reduce the coherent intensity, I_{ri}. The diffuse intensity takes over at larger distances ($\tau > 5$). It is generated by the scattering of the reduced incident intensity in the region of small τ, reaches a maximum near $\tau = 1$ and then decreases again in an exponential fashion. However, the diffuse intensity decreases at a reduced attenuation rate determined in effect by absorption only (though by absorption over multiscattered propagation paths of extended length), while scattering reproduces the diffuse intensity. Hence at large penetration depths, the coherent field component will disappear within the incoherent component, which will determine the received power. In the transition region between the high and low attenuation regimes

significant beam broadening takes place. Thus, it an be expected that in the present case of beam wave pulsed signals, this beam broadening will be accompanied by substantial pulse broadening since both effects are due to multiple scattering. On the other hand, at short distances into the medium where the coherent component dominates, pulse broadening should be minimal except for a certain "filling in" of the deep valleys between adjacent pulses (caused by the incoherent intensity which is small for small τ). The attached figures confirm these trends.

Figure 5 shows satisfaction of the boundary condition that the diffuse intensity $I_{d\upsilon}$ is zero at $\tau = 0$ throughout the forward angular range $0° < \theta < 90°$ (refer to (2.2.7)) for the time-independent case ($\upsilon = 0$). Although not shown, this same result was obtained for values of υ not zero.

As a check on the numerical results, comparisons are made between the data obtained for the case of an incident plane wave pulse train entering a half-space random media using the P_N method in [11] and the current method, referred to as the 2-D Quadrature method. For reference, Figure 6 shows a reproduction of Figure 2 in [11]. Here, the normalized received powers are plotted versus normalized time t' at a normalized penetration depth of $\tau = 1$ for an antenna aligned to receive power in the $\theta_M = 0$, $\phi_M = 0$ direction. Figure 6 also depicts the total normalized received power P' (in dB) as a function of t' at $\tau = 0$, $\tau_\rho = 0$ for scan direction ($\theta_M = 0°$, $\phi_M = 0°$), which equals $f(\tau = 0,\ t')$. This facilitates comparison of what happens to the incident intensity in the random medium as τ increases.

Figures 7a to 7g show, for the plane wave case, the normalized received power (which in this case equals the normalized diffuse received power) at $\tau = 1$ for scan angles of the receive antenna $\theta_M = 4.38°$, $30.02°$, $61.58°$, $86.84°$, $118.42°$, $149.98°$,

175.17° with $\theta_M = 0°$ for N_c = 8, 10, 14. Included in these figures is also the result obtained using the P_N method of [11]. These curves show that agreement is obtained over the most significant portions of the curve, especially at small scan angles, but differ in their relative values in the valley regions where the power is extremely small, or when the scan angle θ_M gets larger, although the shapes of the curves appear to coincide nonetheless. Small antennas scan angles yield the best results and, although agreement improves as N_c increases, the improvement is inconsequential; therefore numerical convergence appears to occur, unless N_c needs to be increased considerably before the level of amplitude values change, which would indicate very slow convergence. It is to be expected that in the limit of very large number of terms in the series solutions, both methods would converge and yield the same result. Due to the high computational intensity of the 2-D Quadrature method, use of very larger values of N_c will result in a considerable increase in computer computational time and is not advisable on the available computer systems. Recall that the 2-D Quadrature method does not allow arbitrary choice of scan angles and, therefore, the reduced incident plus diffuse power is not sampled in the direction $\theta_M = 0°$, $\phi_M = 0°$.

Figure 8 shows, for the plane wave case, the normalized received power (which equals the diffuse received power) versus t' at $\tau = 1$ for scan angles (that are small and nearly equal) $\theta_M = 3.40°$, $4.38°$, $5.52°$ for N_I = 12, 14, 20 with N_c = 8. Again for such small scan angles, agreement is excellent, although for the very small values of power in the valley region, there is a discrepancy in value but not in shape. The same comments made with regard to Figure 7 apply here.

Figures 9 and 10 show the effect of different beamwidths. In Figure 9, the received power P' versus time t' is plotted at $\tau = 1$ for the scan direction ($\theta_M = 4.38°$, $\phi_M = 0°$)

and for normalized beamwidths $w' = $ 0.5, 1, 3, 5 using the 2-D Quadrature method as well as the plane wave case ($w' \to \infty$) at $\tau = 1$ using both the Quadrature and the P_N methods. Note that the leading flanks of the pulses suffer little distortion while the trailing flanks are broadened out substantially, particularly for the small beamwidth. As explained in [11] for the plane wave case, this is explained by observing that pulse broadening is caused primarily by the delayed arrival of multiscattered waves trains that travel over paths of extended lengths, thus producing the "tails" of the received pulses. Note also that for $w' \gg \tau$ the beam wave case approaches the plane wave case, as was expected.

Figures 11a and 11b for beamwidths $w' = $ 1 and 5, respectively, depict the total received power P' (which equals the diffuse received power) versus time t' for different penetration depths $\tau = $ 1, 3, 5 and 10 for the small scan direction ($\theta_M = 4.38°$, $\phi_M = 0°$). The figures also include the plane wave cases ($w' \to \infty$) at $\tau = 1$ calculated using both the Quadrature and the P_N methods. At the larger values of penetration depth, the power is seen to attenuate and the pulse width to increase with the attendant pulse distortion due to the overlap of adjacent pulses, (although only slightly for $\tau = $ 1, 3, 5 but significantly for $\tau = 10$).

Finally, Figures 12a and 12b provide a comparison of the received power versus time t' for three scan directions, $\theta_M = 4.38°$, 17.40°, 30.02° with $\phi_M = 0°$ at $\tau = 1, 5$ and for $w' = 1$. Note that as θ_M increases, the beam wave pulse train exhibits more attenuation and pulse broadening and distortion particularly at $\tau = 5$, although the overall shapes of the pulses remain similar.
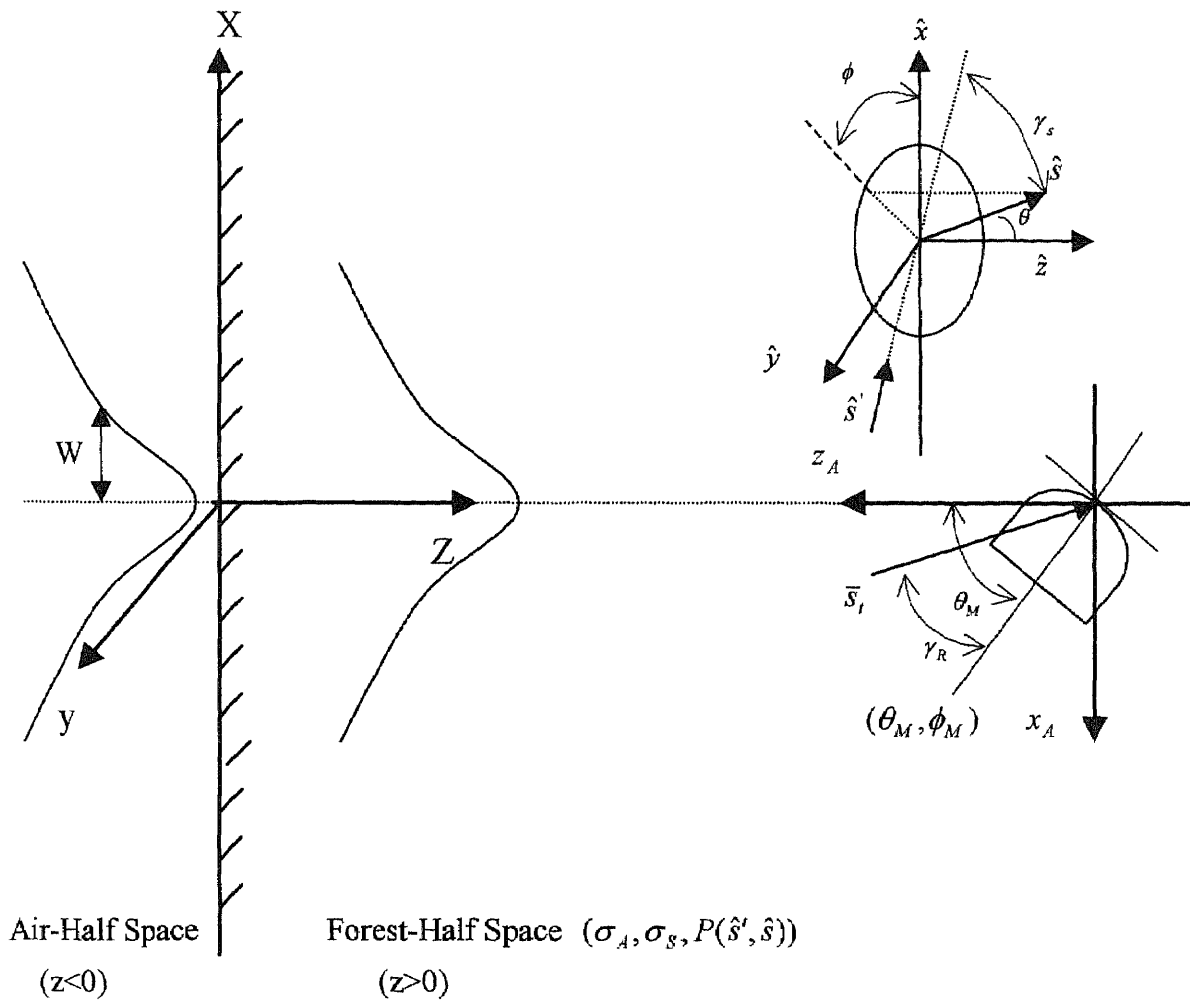
Figure 1 Geometry of a beam wave pulse train normally incident on a semi-infinite medium and receiving antenna.
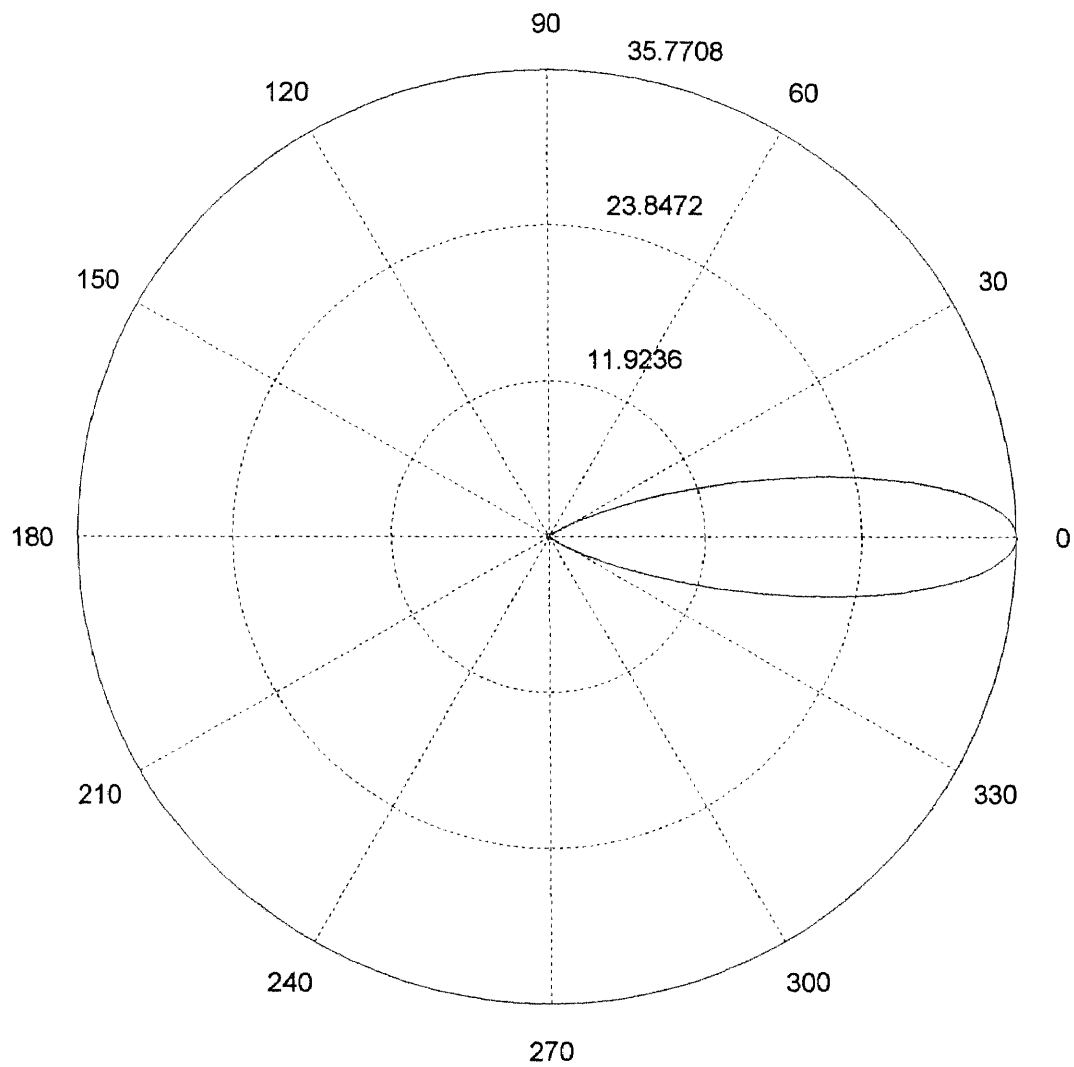
Figure 2 Gaussian scatter (phase) function.
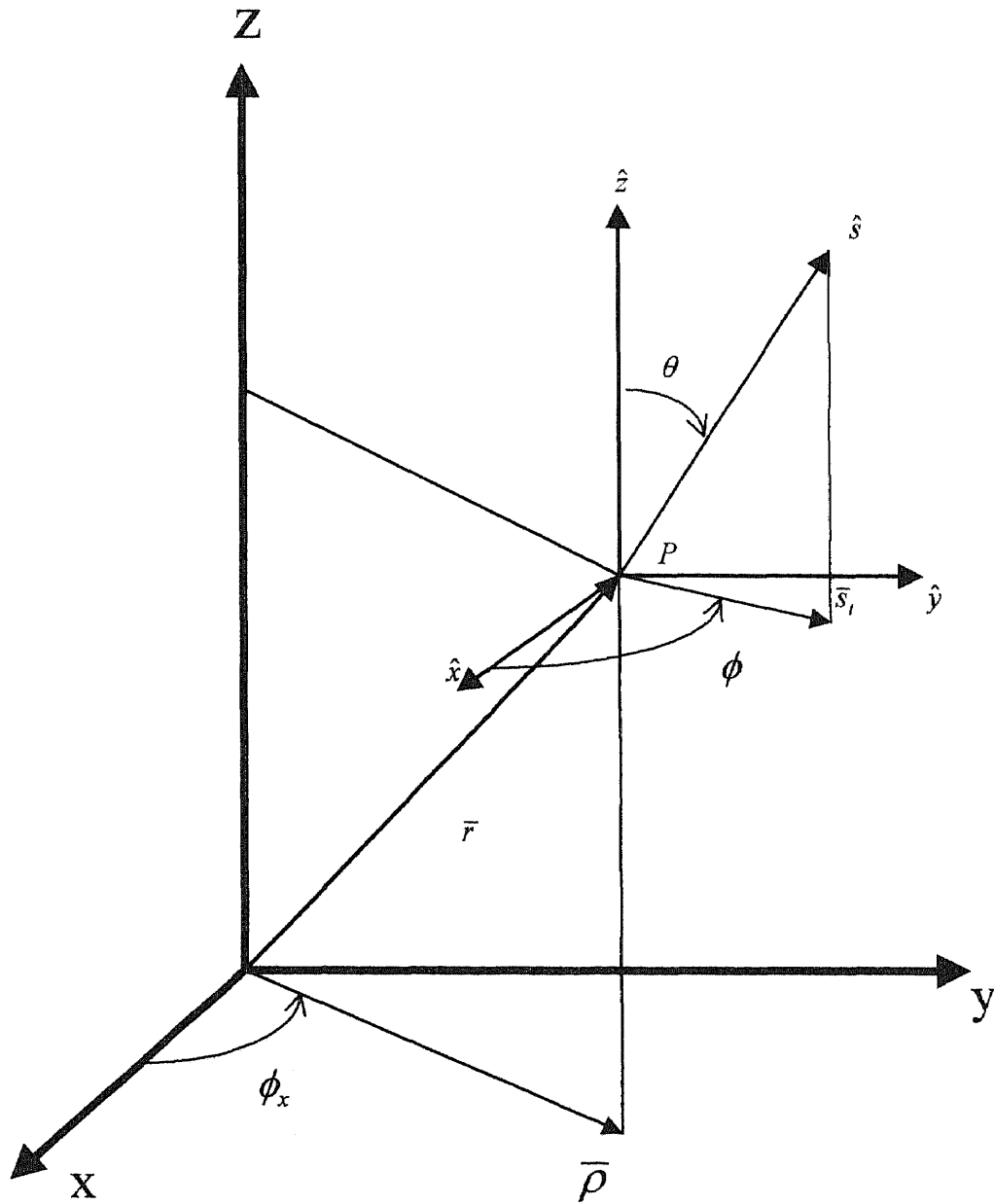
Figure 3 Variables for the specific intensity in the cylindrical coordinate system at the point $P(r, \theta, \phi_x)$.
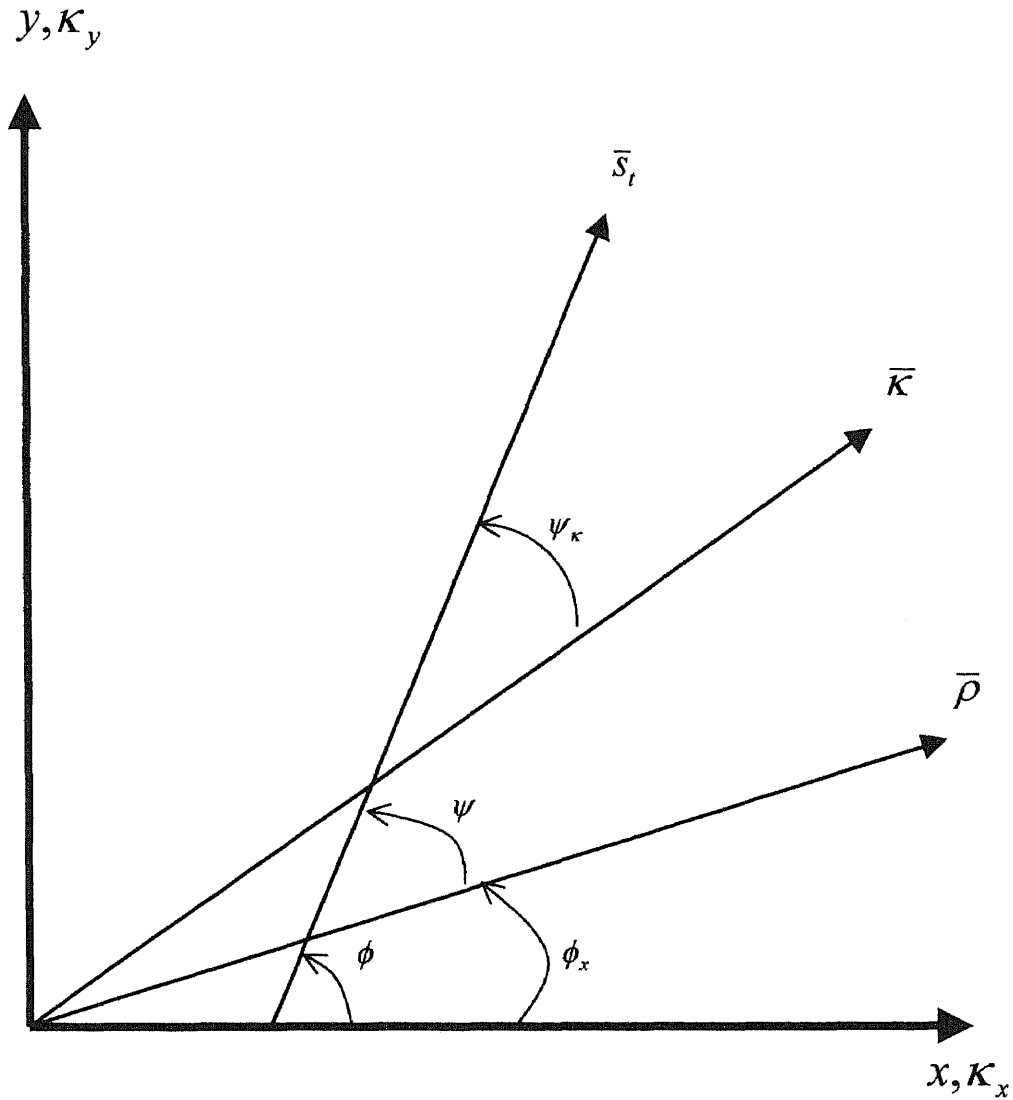
Figure 4 The azimuthal angles ψ and ψ_κ and their relation to the $\bar{s}_t$, $\bar{\kappa}$ and $\bar{\rho}$ vectors. Note that $\psi = \phi - \phi_x$.
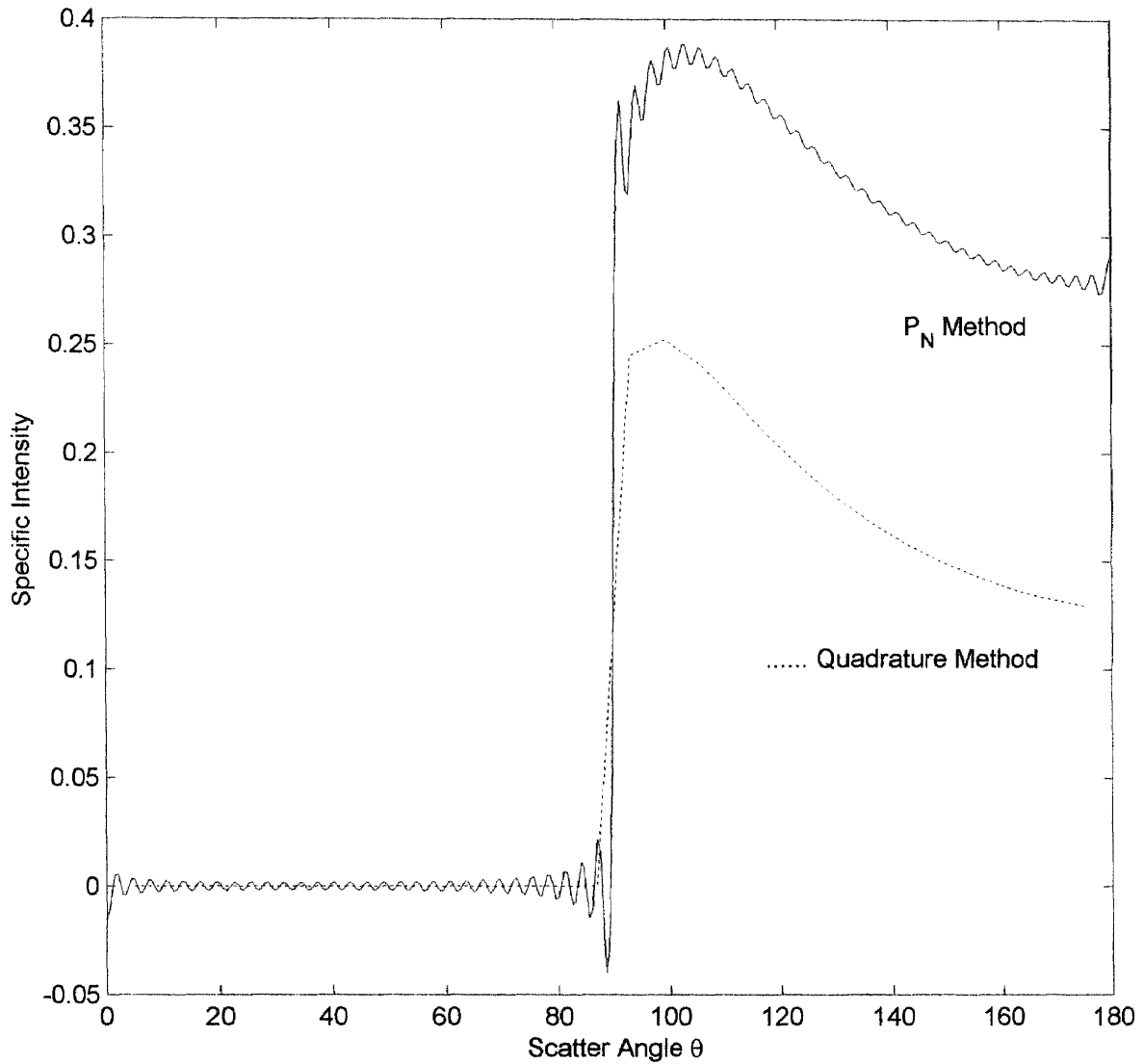
Figure 5 Boundary condition for the time-independent plane wave case, specific intensity I_{d0} at $\tau = 0$ versus scatter angle θ. Using both P_N Method ($N = 121$) and 2-D Quadrature Method ($N_l = 14$, $N_c = 8$).
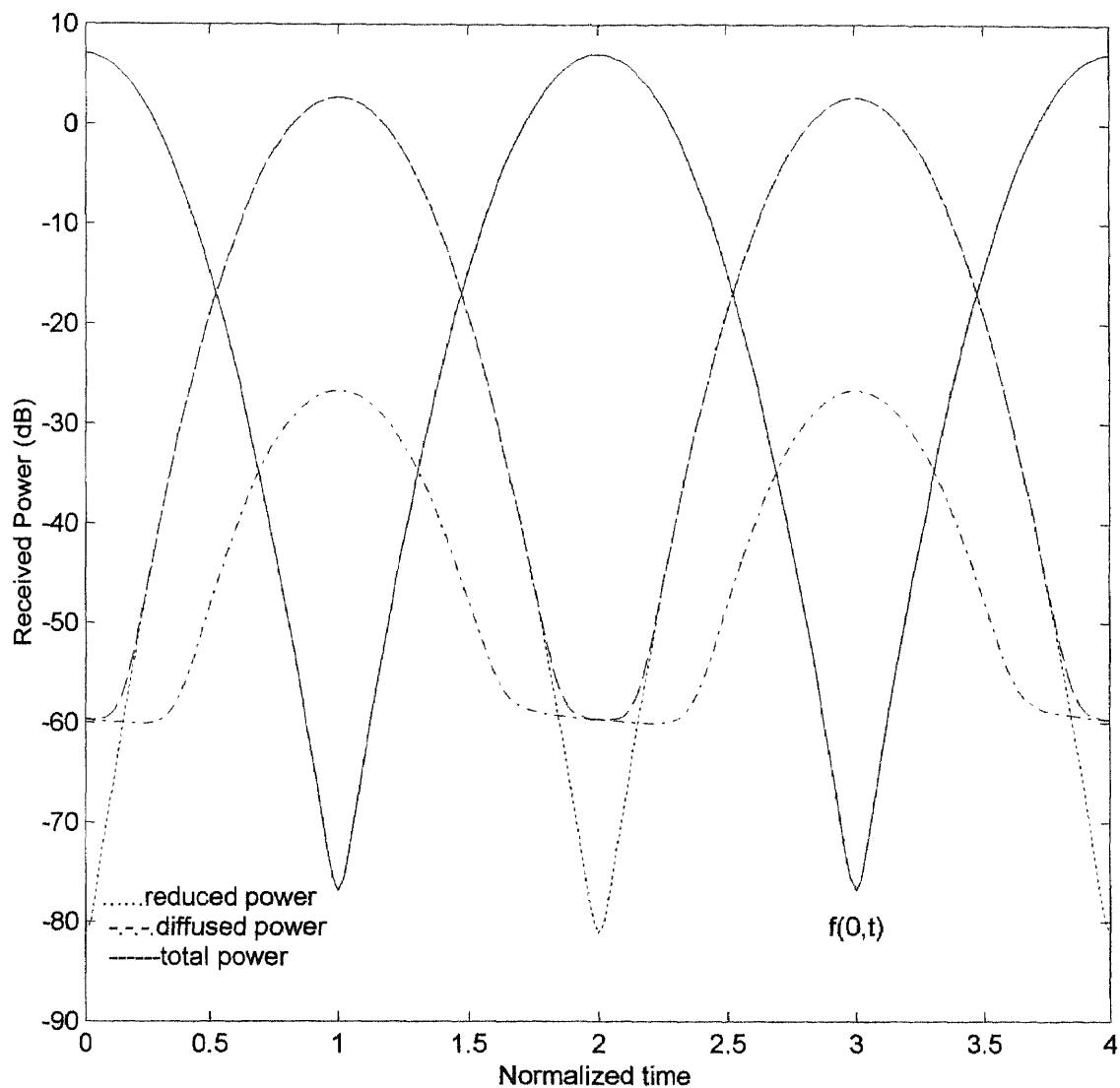
Figure 6 Normalized received powers (by P_N Method) P', P'_{ri}, P'_d at $\tau = 1.0$ versus normalized time t' for $W_o = 0.75$, $\Delta\gamma_s = 0.3$ rad, $\Delta\gamma_M = 0.012$ rad, $N = 121$, $T' = 2.0$, $\alpha = 0.8$, $\theta_M = 0°$, $\theta_P = 0°$. Also shown (for reference) is $f(0,t')$ or normalized received power $P'(0,t',0)$ in dB versus normalized time t'.
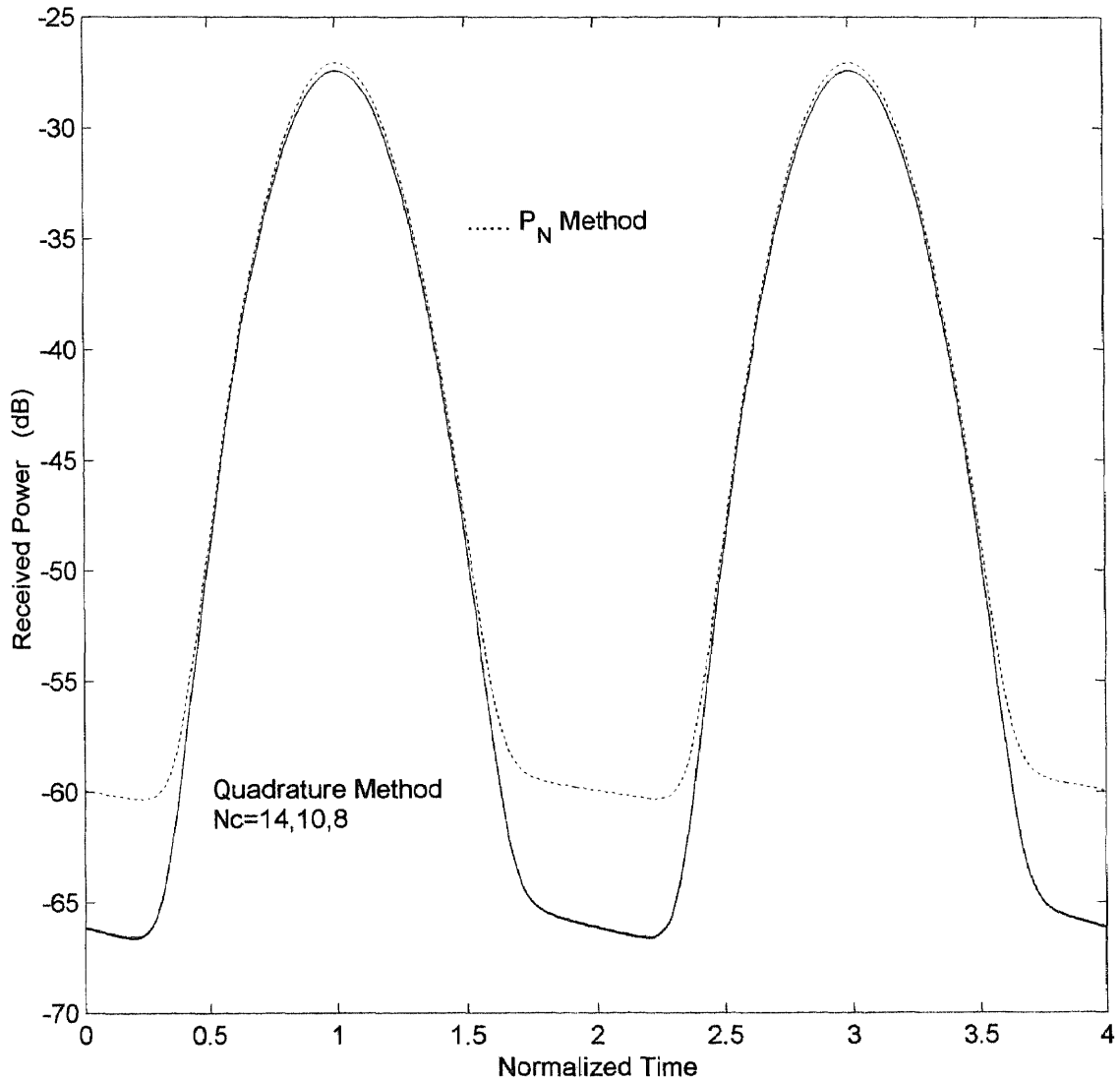
Figure 7a Normalized received powers P' at $\tau = 1.0$ versus normalized time t' for $N_I = 14$, $N_c = 8, 10, 14$, $\theta_M = 4.83°$, and beamwidth $w' = \infty$ (plane wave case). P' generated by P_N Method (plane wave case) is also shown as a reference.
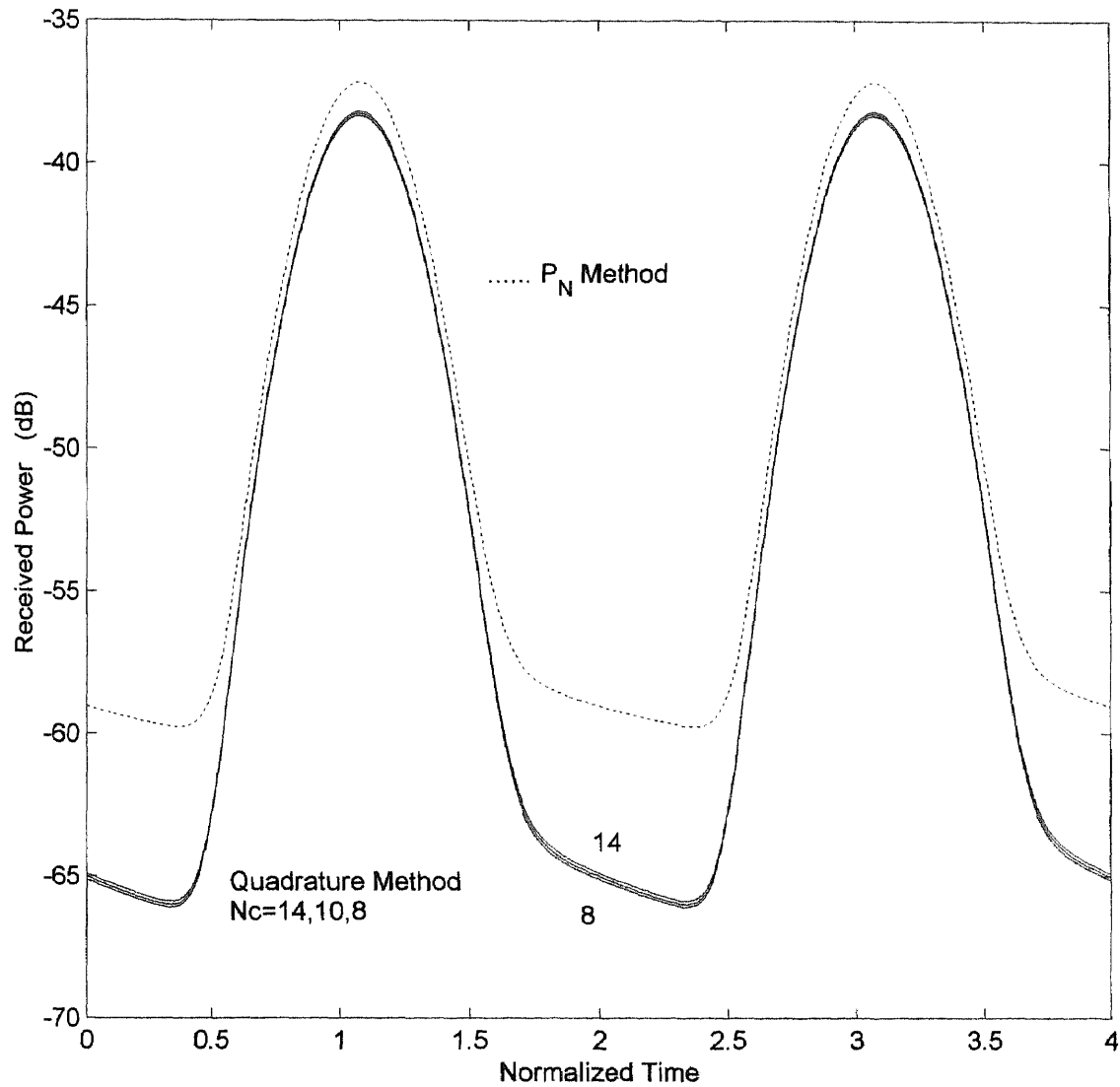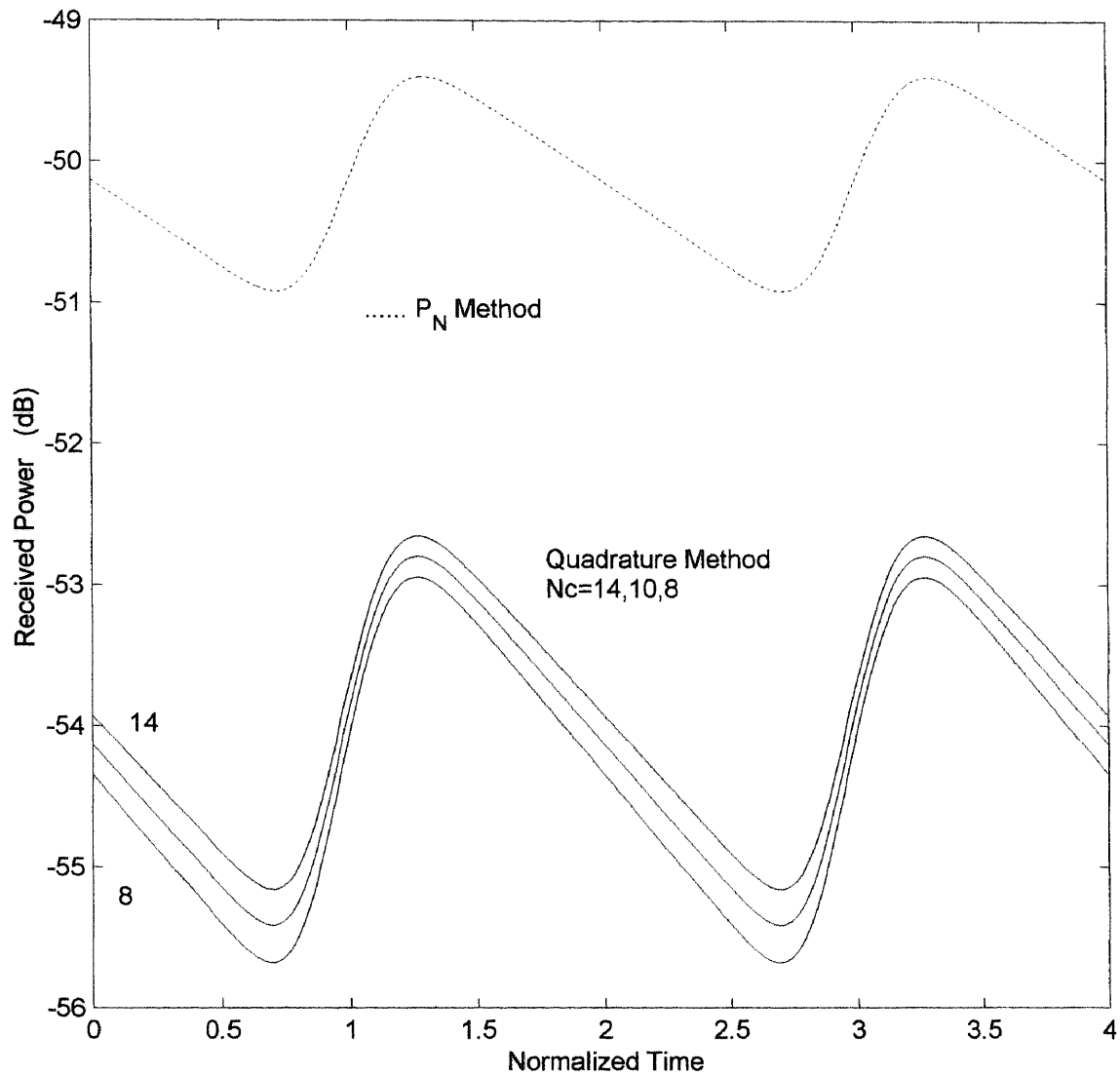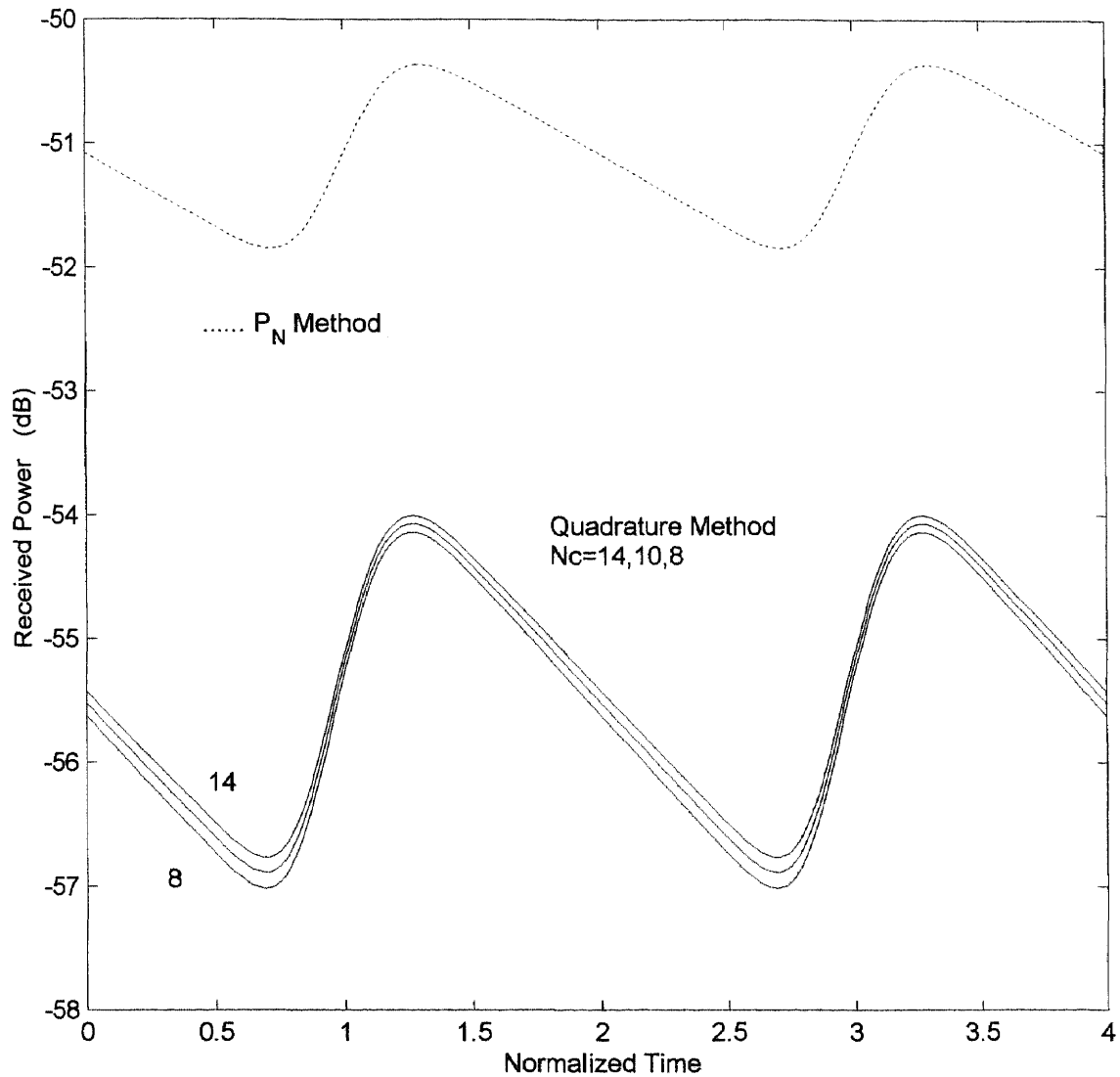
Figure 7b Normalized received powers P' at $\tau = 1.0$ versus normalized time t' for $N_I = 14$, $N_c = 8, 10, 14$, $\theta_M = 30.01°$, and beamwidth $w' = \infty$ (plane wave case). P' generated by P_N Method (plane wave case) is also shown as a reference.
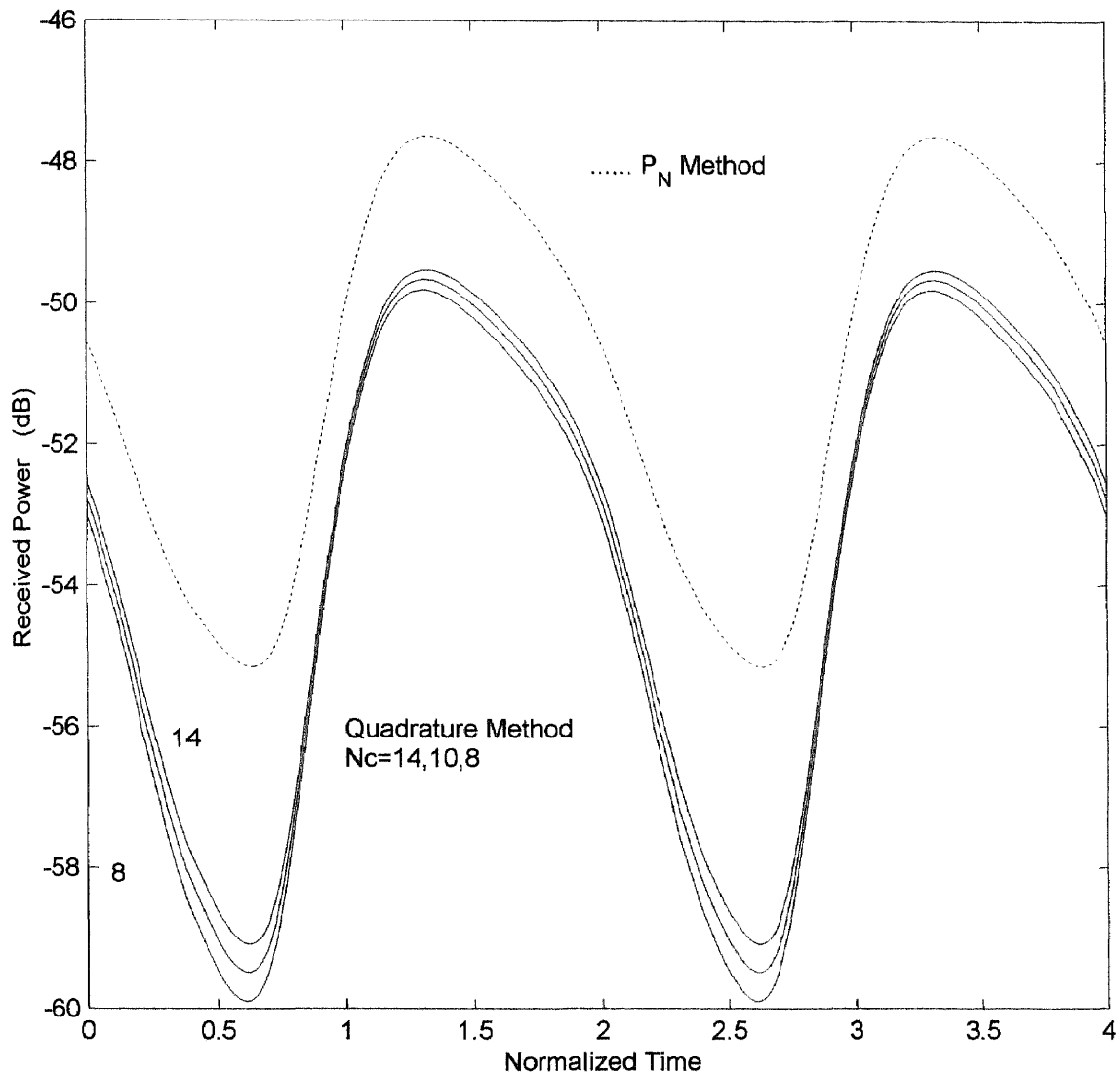
Figure 7c Normalized received powers P' at $\tau = 1.0$ versus normalized time t' for $N_l = 14$, $N_c = 8, 10, 14$, $\theta_M = 61.58°$, and beamwidth $w' = \infty$ (plane wave case). P' generated by P_N Method (plane wave case) is also shown as a reference.
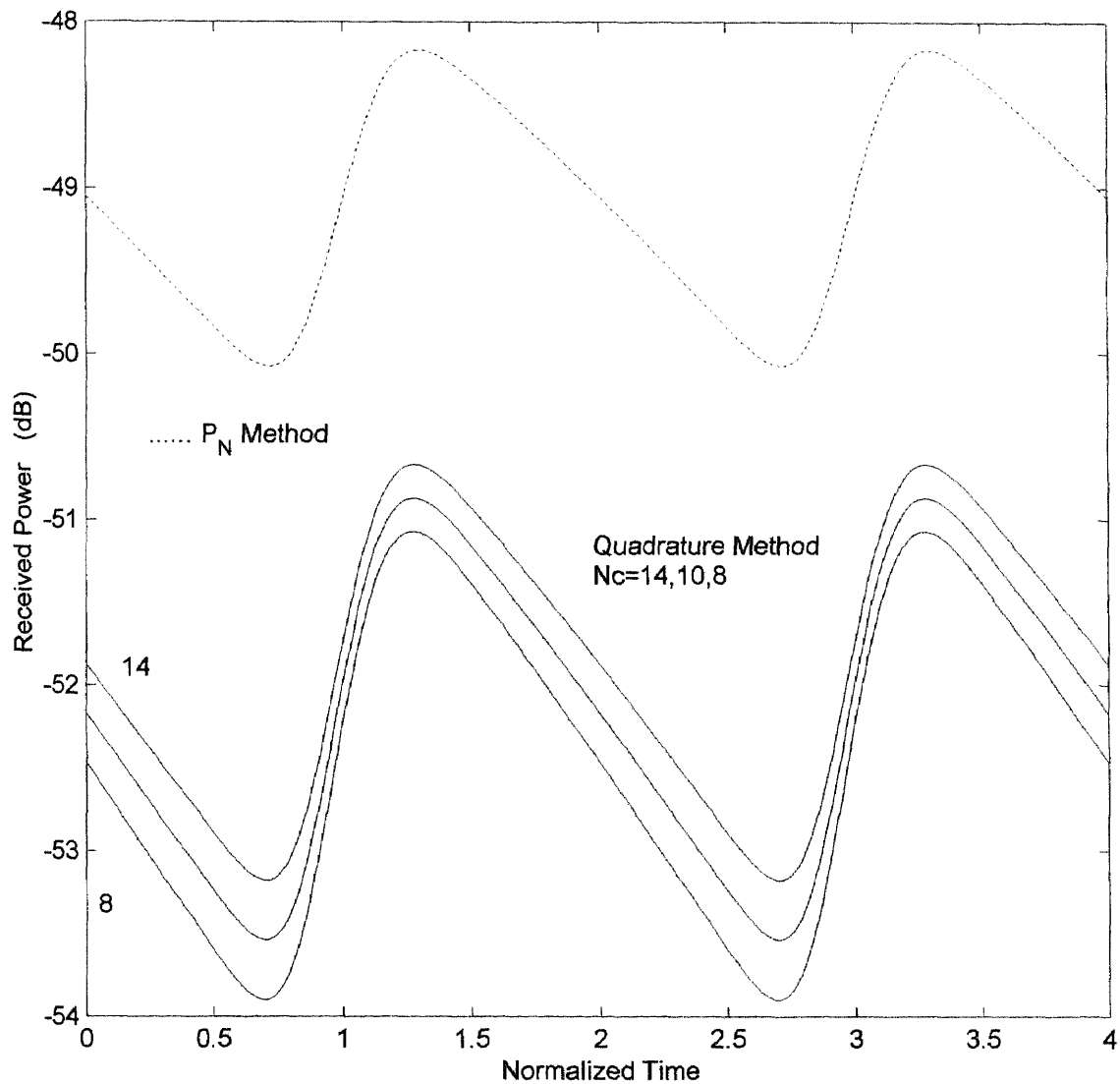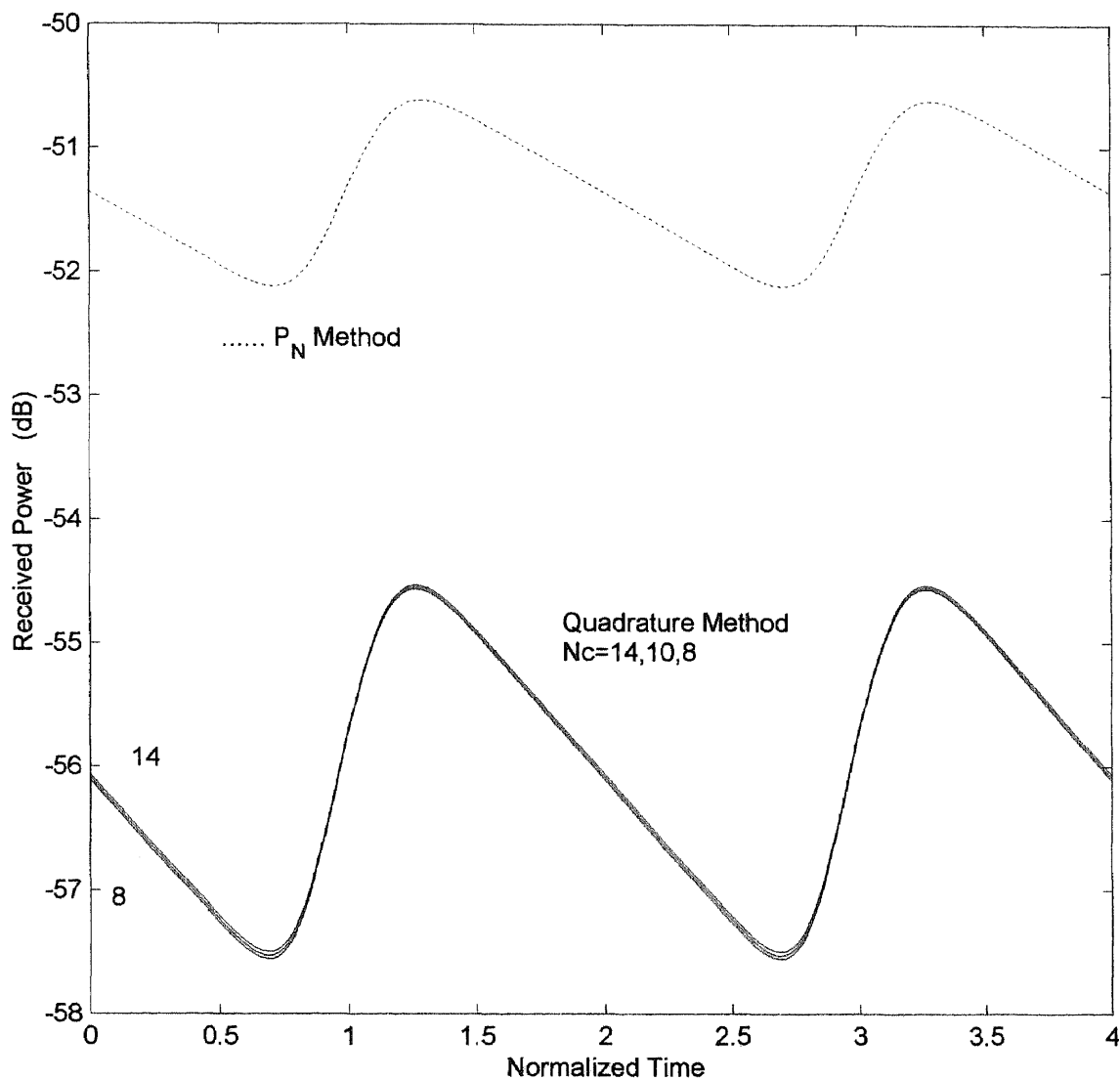
Figure 7d Normalized received powers P' at $\tau = 1.0$ versus normalized time t' for $N_I = 14$, $N_c = 8, 10, 14$, $\theta_M = 86.84°$, and beamwidth $w' = \infty$ (plane wave case). P' generated by P_N Method (plane wave case) is also shown as a reference.
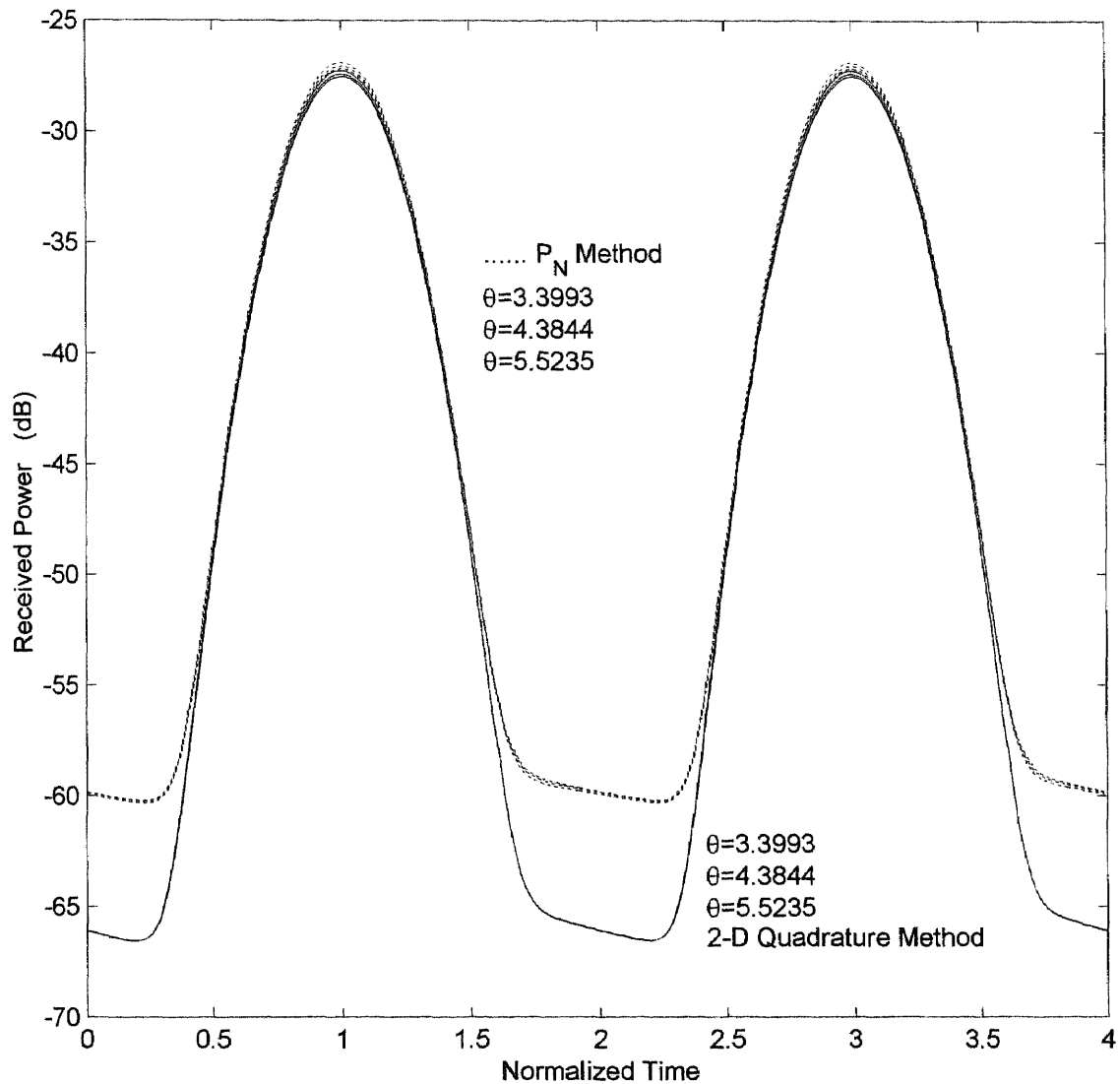
Figure 7e Normalized received powers P' at $\tau = 1.0$ versus normalized time t' for $N_I = 14$, $N_c = 8, 10, 14$, $\theta_M = 118.42°$, and beamwidth $w' = \infty$ (plane wave case). P' generated by P_N Method (plane wave case) is also shown as a reference.
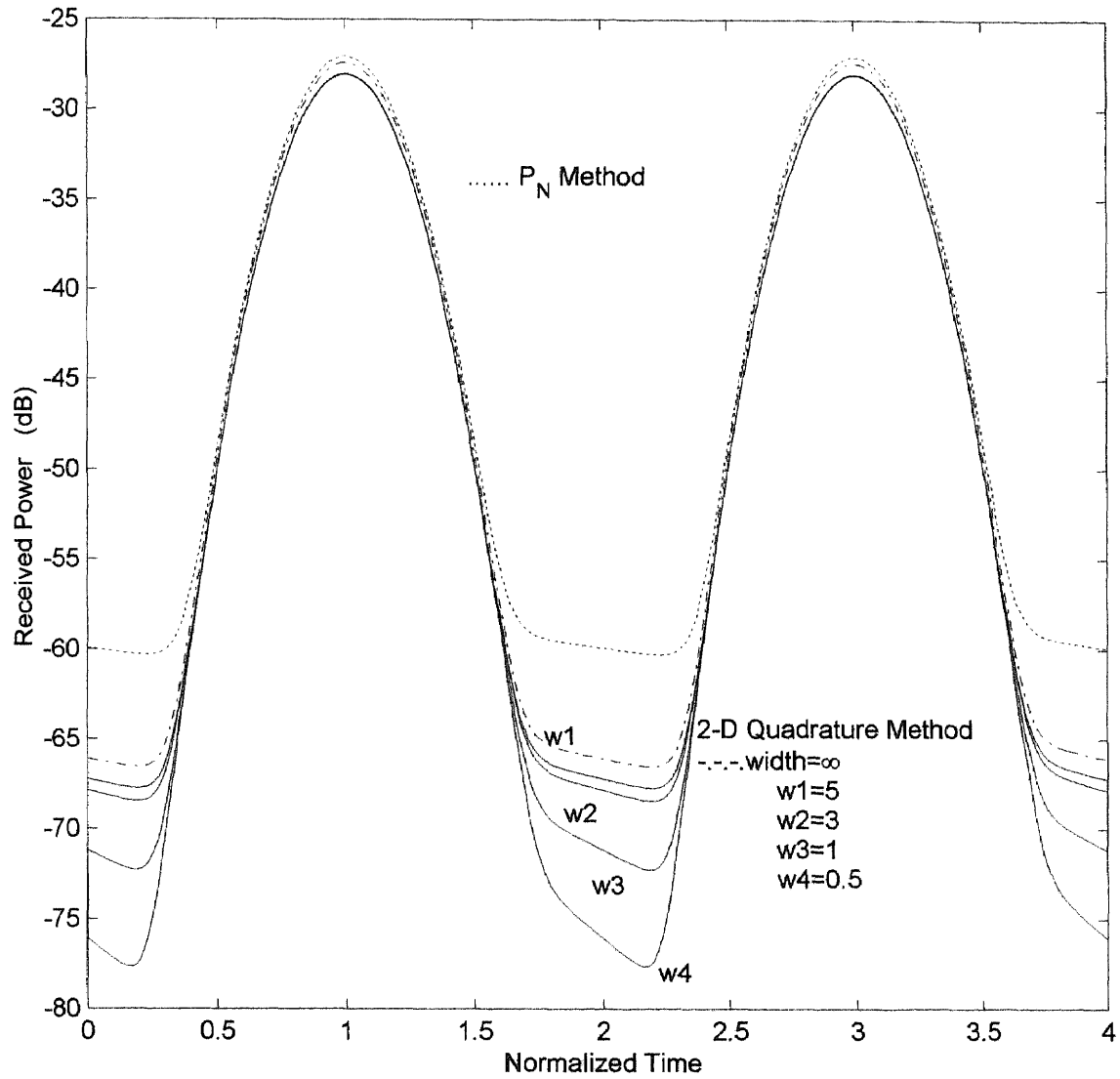
Figure 7f Normalized received powers P' at $\tau = 1.0$ versus normalized time t' for $N_l = 14$, $N_c = 8, 10, 14$, $\theta_M = 149.98°$, and beamwidth $w' = \infty$ (plane wave case). P' generated by P_N Method (plane wave case) is also shown as a reference.
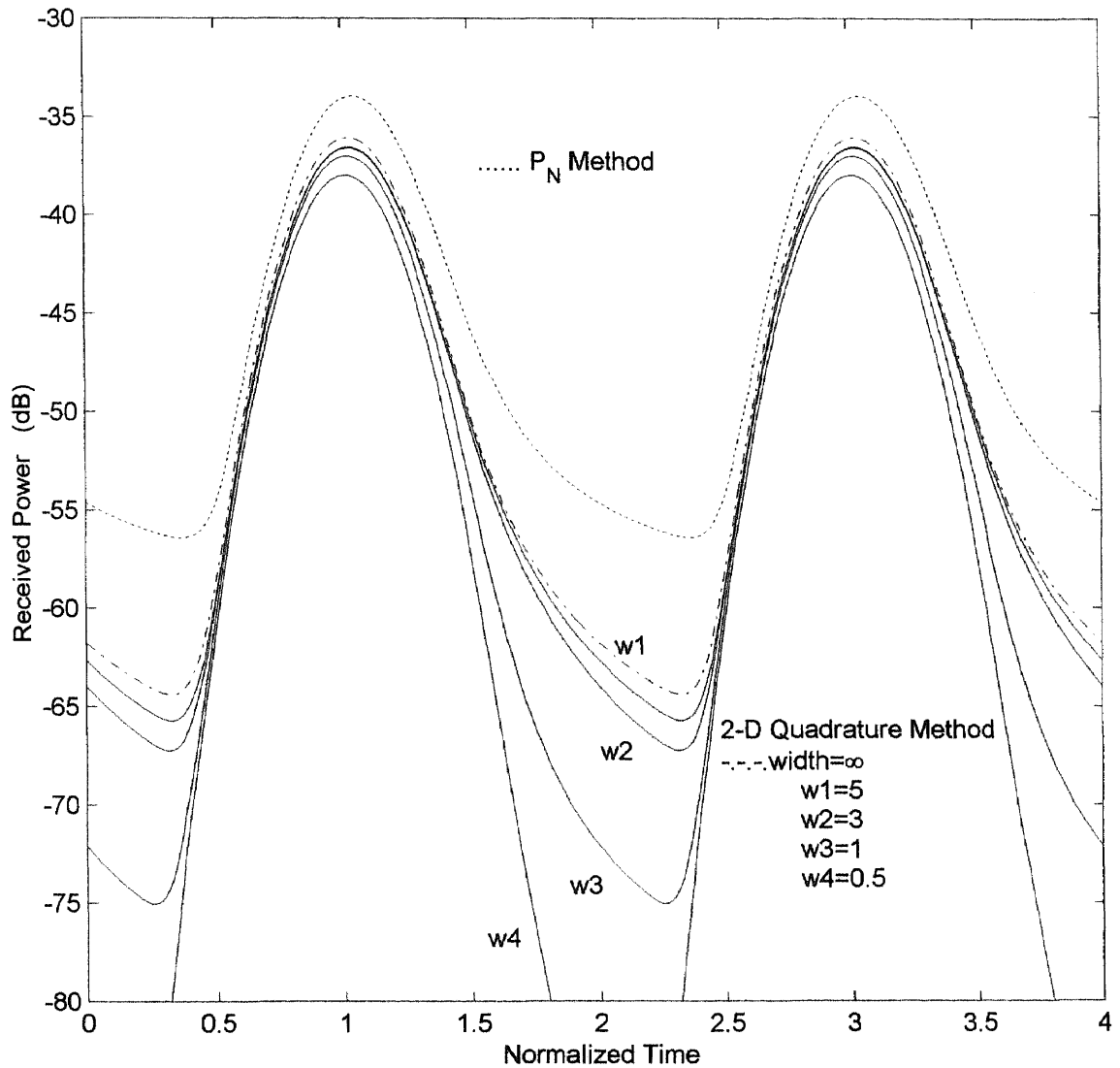
Figure 7g Normalized received powers P' at $\tau = 1.0$ versus normalized time t' for $N_I = 14$, $N_c = 8, 10, 14$, $\theta_M = 175.17°$, and beamwidth $w' = \infty$ (plane wave case). P' generated by P_N Method (plane wave case) is also shown as a reference.

Figure 8 Normalized received powers P' at $\tau = 1.0$ versus normalized time t' for $N_l = 12, 14, 20$, $N_c = 8$, $\theta_M = 3.40°(N_l = 20)$, $4.38°(N_l = 14)$, $5.52°(N_l = 12)$, and beamwidth $w' = \infty$. P' generated by P_N Method (plane wave case) is also shown as a reference.

Figure 9a Normalized received powers P' at $\tau = 1.0$ versus normalized time t' for $N_l = 14$, $N_c = 8$, $\theta_M = 4.38°$, and beamwidth $w' = 0.5$, 1, 3, 5, ∞. P' generated by P_N Method (plane wave case) is also shown as a reference.
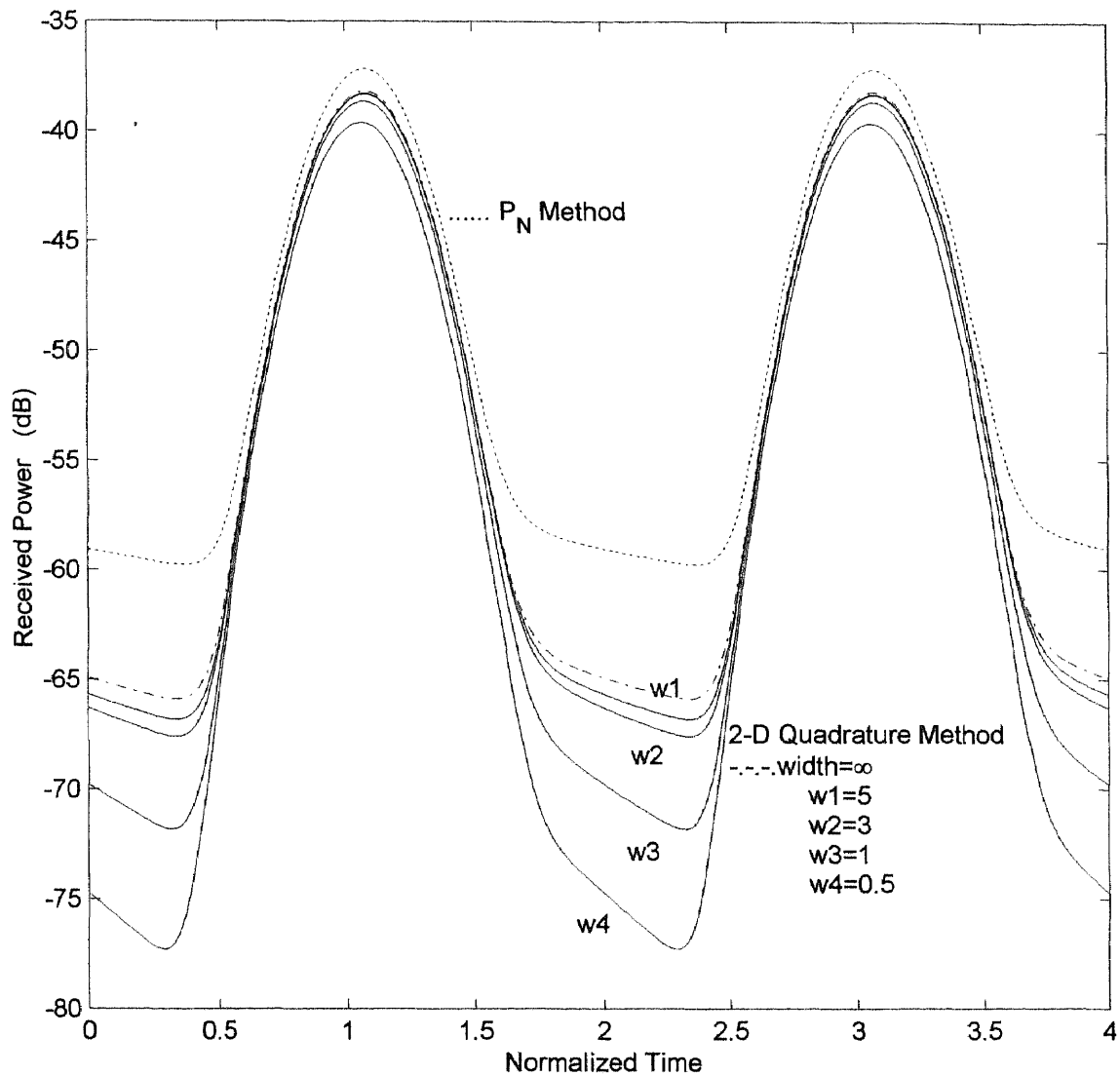
Figure 9b Normalized received powers P' at $\tau = 5.0$ versus normalized time t' for $N_l = 14$, $N_c = 8$, $\theta_M = 4.38°$, and beamwidth $w' = 0.5, 1, 3, 5, \infty$. P' generated by P_N Method (plane wave case) is also shown as a reference.
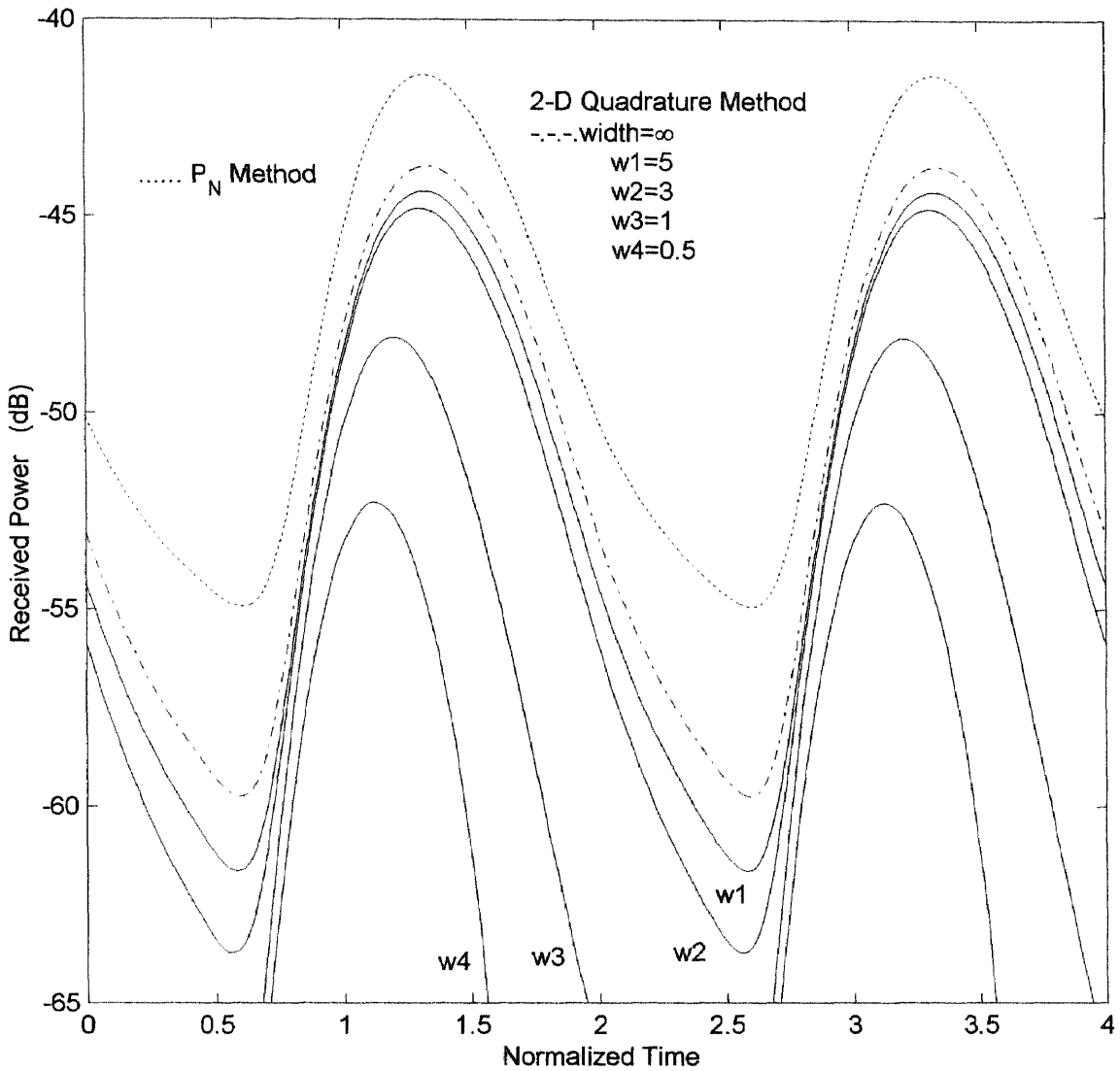
Figure 10a Normalized received powers P' at $\tau = 1.0$ versus normalized time t' for $N_I = 14$, $N_c = 8$, $\theta_M = 30.15°$, and beamwidth $w' = 0.5$, 1, 3, 5, ∞. P' generated by P_N Method (plane wave case) is also shown as a reference.

Figure 10b Normalized received powers P' at $\tau = 5.0$ versus normalized time t' for $N_I = 14$; $N_c = 8$, $\theta_M = 30.15°$, and beamwidth $w' = 0.5, 1, 3, 5, \infty$. P' generated by P_N Method (plane wave case) is also shown as a reference.
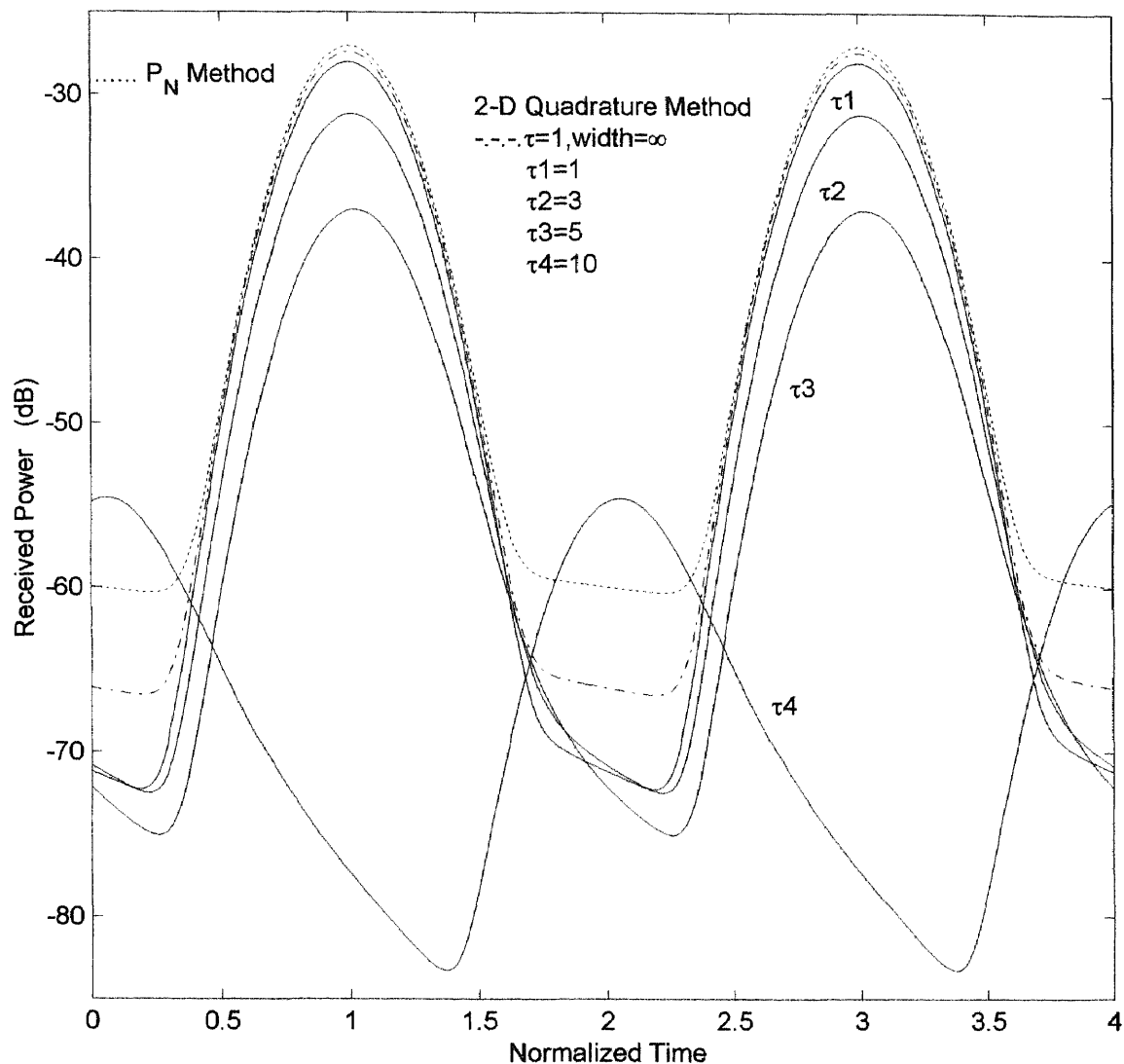
Figure 11a Normalized received powers P' at $\tau = 1, 3, 5,$ and 10 versus normalized time t' for $N_I = 14$, $N_c = 8$, $\theta_M = 4.38°$, and beamwidth $w' = 1$. P' generated by P_N Method and 2-D Quadrature Method with $\tau = 1$, $w = \infty$ (plane wave cases) are also shown as a reference.
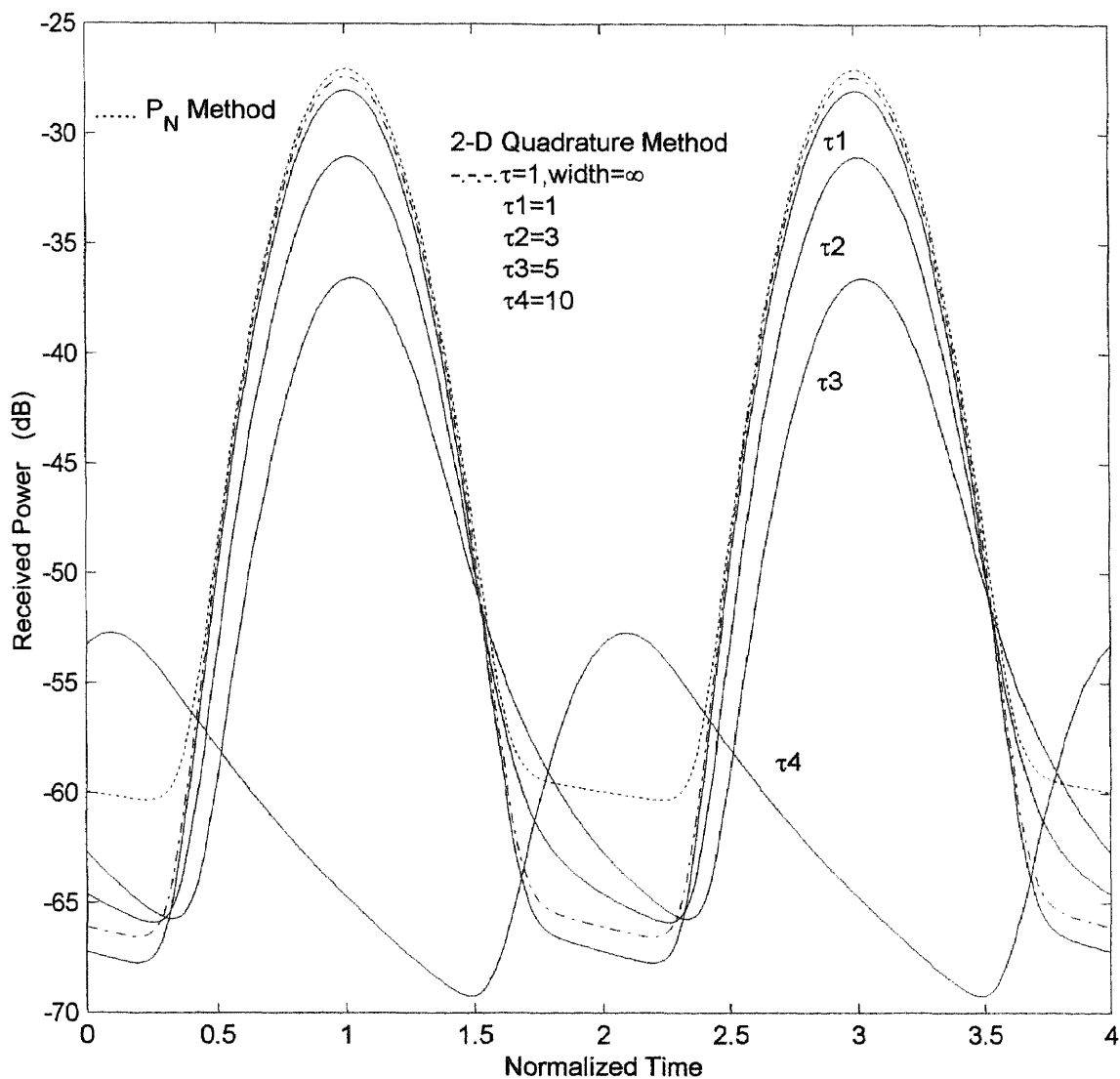
Figure 11b Normalized received powers P' at $\tau = 1, 3, 5,$ and 10 versus normalized time t' for $N_I = 14$, $N_c = 8$, $\theta_M = 4.38°$, and beamwidth $w' = 5$. P' generated by P_N Method and 2-D Quadrature Method with $\tau = 1$, $w = \infty$ (plane wave cases) are also shown as a reference.
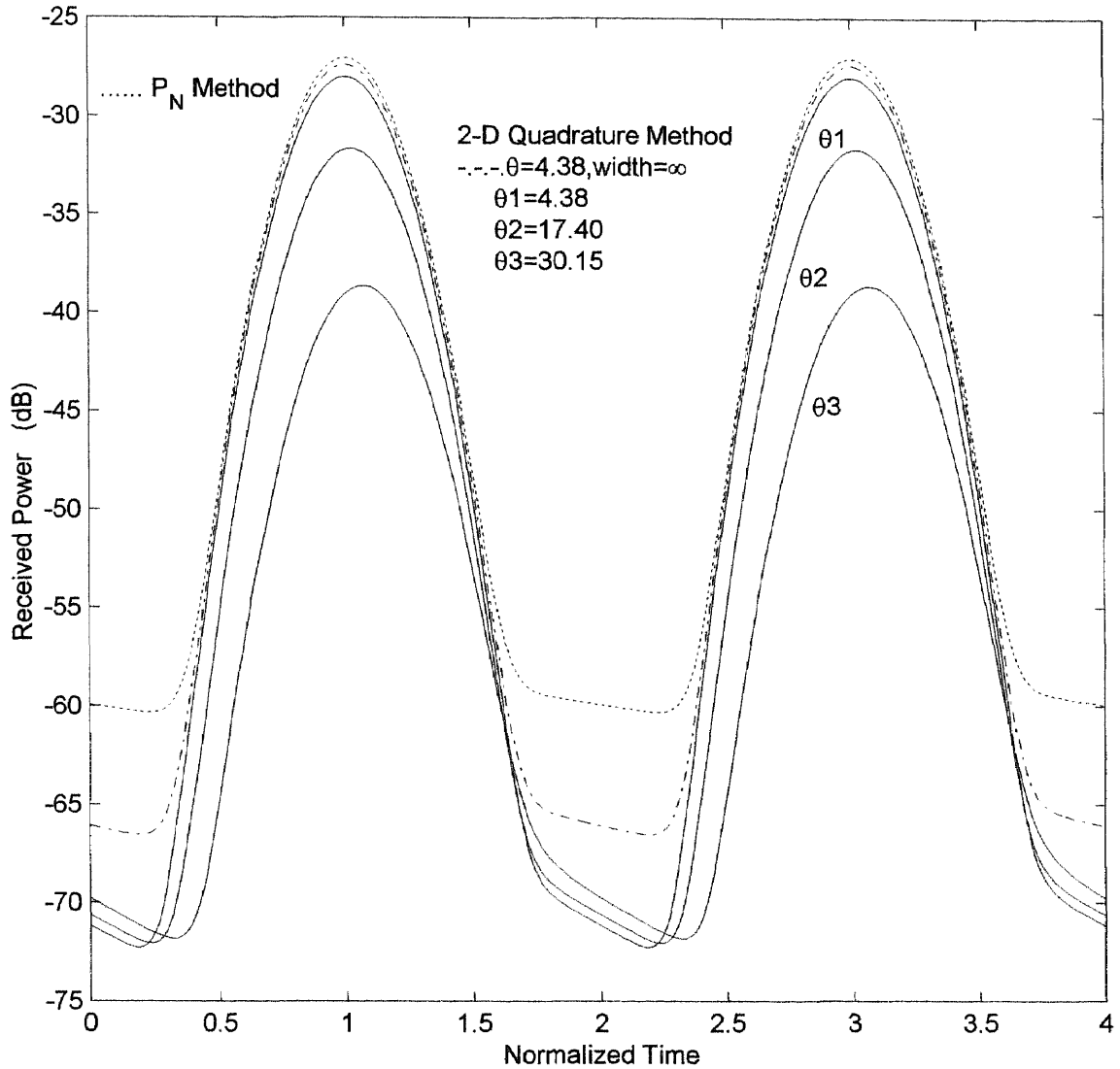
Figure 12a Normalized received powers P' at $\tau = 1$ versus normalized time t' for $N_I = 14$, $N_c = 8$, $\theta_M = 4.38°$, $17.39°$, $30.02°$ and beamwidth $w' = 1$. P' generated by P_N Method and 2-D Quadrature Method with $\theta_M = 4.38°$, $w' = \infty$ (plane wave cases) are also shown as a reference.

Figure 12b Normalized received powers P' at $\tau = 5$ versus normalized time t' for $N_I = 14$, $N_c = 8$, $\theta_M = 4.38°$, $17.39°$, $30.02°$ and beamwidth $w' = 1$. P' generated by P_N Method and 2-D Quadrature Method with $\theta_M = 4.38°$, $w' = \infty$ (plane wave cases) are also shown as a reference.
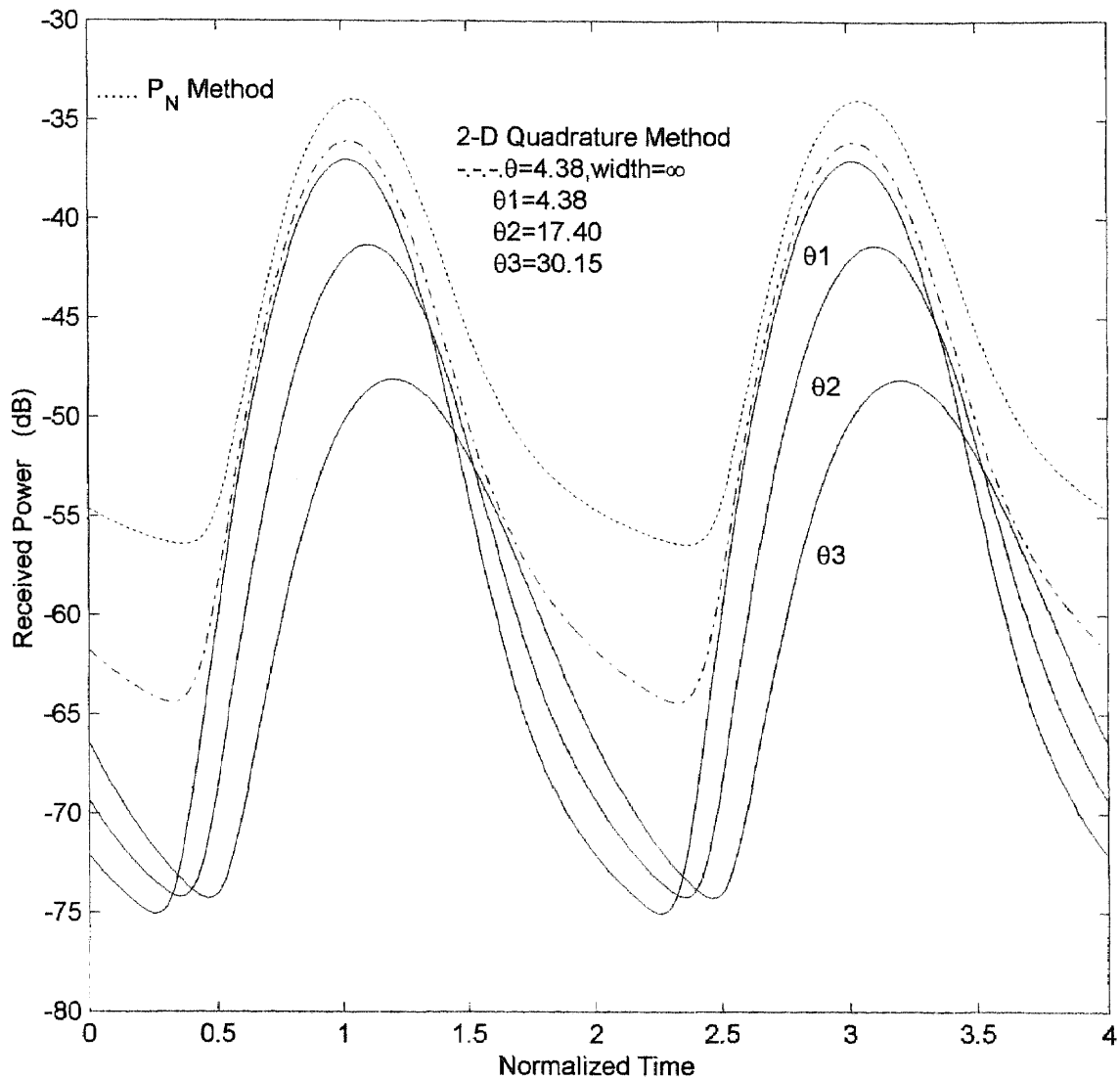
CHAPTER 6

CONCLUSIONS AND SUGGESTIONS

The 2-D Quadrature method of solution to the scalar time-dependent transport equation is used to study beam wave narrow band pulse propagation in a random medium of discrete scatters. A bounded beam wave pulse train is assumed to normally enter the medium which is modeled as a slab or half-space region consisting of a statistically homogeneous, random distribution of particles which produces strong forward scattering. The averaged scatter (phase) function of the medium is assumed to consist of a narrow forward lobe (assumed to be Gaussian) superimposed on an omnidirectional background. The time-dependent scalar transport equation is solved for both the coherent (reduced incident) and the incoherent (diffuse) field intensities. Four parameters characterize the propagation, scattering and absorption properties of the medium. The theory is useful in particular for the description of collimated millimeter-wave pulse propagation effects in woods and forests as well as for optical beams in the atmosphere.

Plots of the received power in the random medium (forest) showed pulse broadening effects and the power attenuation, especially at large penetration depths. Comparison with a second completely different method of solution, called the P_N method, to the scale transport equation substantiated the results for the special care of an incident plane wave pulse train in relatively small scan angles and small penetration depths. Work in progress includes the development of more analytical methods of solution to the problems of scattering of bounded and divergent beam wave pulse trains in a random medium that is characterized by a scatter function with a strong forward lobe superimposed on an isotropic background.

APPENDIX A

2-D GAUSS QUADRATURE FORMULA

In the discussion of the bounded beam-wave pulse train problem, two coupled integro-differential equations are solved. As in [12], these equations are converted to a system of differential equations, which are then solved by using an eigenvalue-eigenvector technique. In converting to a system of differential equations, the double integral terms are approximated by summations. In this appendix, the technique known as 2-D Gaussian quadrature is presented and used to evaluate the double integrals. Most of this discussion can be found in [1, 9, and 16].

The numerical quadrature formula for an integral of the form

$$\int_{-1}^{1} f(x)dx = \sum_{i=1}^{n} w_i^l f(x_i^l) + R_n^l \tag{A.1}$$

is known as the Gauss-Legendre formula. The variables x_i^l and w_i^l are, respectively, the abscissas and weights, where x_i^l is the ith zero of Legendre polynomial $P_n(x)$

and
$$w_i^l = \frac{2}{(1 - x_i^{l^2})P_n'(x_i^l)^2} \quad , \quad i = 1, 2 \cdots n \quad . \tag{A.1a}$$

and $P_n'(x)$ is the derivative of $P_n(x)$.

The error term R_n^l is specified by the following relation

$$R_n^l = \frac{2^{2n+1}(n!)^4}{(2n+1)[(2n)!]^3} f^{2n}(\xi) \quad , \quad -1 < \xi < 1 \quad . \tag{A.1b}$$

Similarly, the numerical quadrature formula for an integral of the form

$$\int_{-1}^{1} \frac{f(x)}{\sqrt{1-x^2}}dx = \sum_{j=1}^{m} w_j^c f(x_j^c) + R_m^c \tag{A.2}$$

is the Gauss-Chebyshev formula. The abscissas and weights are

$$x_j^c = \cos\left[\frac{(2j-1)\pi}{2m}\right] \quad , \quad w_j^c = \frac{\pi}{m} \quad . \tag{A.2a}$$

The error term in this case takes the form

$$R_m^c = \frac{2\pi}{2^{2m}(2m)!} f^{2m}(\xi) \quad , \quad -1 < \xi < 1. \tag{A.2b}$$

Let $h(\theta,\phi)$ be any function defined on a hemisphere. The east hemisphere is chosen, i.e.,

$$0 \le \theta \le \pi \quad , \quad 0 \le \phi \le \pi. \tag{A.3}$$

Since spherical functions are usually expanded in terms of Legendre polynomials $P_n(\cos\theta)$ and $e^{im\phi}$, they are polynomials in $\cos\theta$ and $\cos\phi$. As a result, the 2-D spherical integral below can be approximated by first making the change of variables

$$\mu = \cos\theta \quad , \quad \alpha = \cos\phi \tag{A.4}$$

and then using both (A.1) and (A.2) as follows

$$\int_0^\pi \int_0^\pi h(\theta,\phi)\sin\theta\, d\phi\, d\theta = \int_0^\pi \int_0^\pi \frac{h(\mu,\alpha)}{\sqrt{1-\alpha^2}} d\alpha\, d\mu$$
$$\approx \sum_{i=-N_l}^{N_l} w_i^l \left\{ \sum_{j=1}^{N_c^l} w_{i,j}^c h(\mu_i^l, \alpha_{i,j}^c) \right\}, \tag{A.5}$$

where the abscissas and weights are defined above, identified by the superscripts " l " and " c ". In addition, the abscissas and weights satisfy the conditions

$$\mu_{-i}^l = -\mu_i^l \quad , \quad w_{-i}^l = w_i^l$$
$$N_c^{-i} = N_c^i \quad , \quad \alpha_{-i,j}^c = \alpha_{i,j}^c \tag{A.6}$$
$$w_{i,j}^c = \frac{\pi}{N_c^i} \cdot$$

As in [9], a varying order for the Gauss-Chebyshev integration is used so that the size of the matrix could be controlled in the computer program.

Using the above results and keeping in mind the format of the matrix equation in Chapter 3, the integral terms in (3.1.12a and 12b) (see also (3.2.5)) take the form of the equation

$$\int_0^\pi \int_0^\pi h(\theta,\phi)\sin\theta\, d\phi\, d\theta \approx \sum_{\substack{q=-N \\ q\neq 0}}^{N} w_q P_S(\mu,\alpha,\mu_q,\alpha_q) I_{x\upsilon}(\mu,\alpha,\mu_q,\alpha_q) \tag{A.7}$$

APPENDIX B

POWER RECEIVED BY A HIGHLY DIRECTIVE ANTENNA

In this study of beam wave pulses normally incident on a semi-infinite medium, the power is assumed to be received by a highly directive antenna placed in the forest. The power calculations were introduced in [8, 11] and are repeated here for convenience.

Assume that a highly directive, lossless antenna of narrow beamwidth and narrow bandwidth is located inside the forest. This receiving antenna is characterized by an effective aperture $A(\gamma_R)$, where γ_R is the angle included between the direction of observation (θ_R, ϕ_R) and the pointing direction of the antenna axis, i.e., the main beam direction (θ_M, ϕ_M); see Figure 3. Hence,

$$\cos \gamma_R = \cos \theta_R \cos \theta_M + \sin \theta_R \sin \theta_M \cos(\phi_R - \phi_M) . \tag{B.1}$$

In transport theory powers add. Hence, the instantaneous power received by the antenna is the sum of the intensity contributions coming from all directions multiplied by the effective aperture of the antenna, i.e.,

$$P_R^{tot}(\tau, \tau_\rho, t', \theta_M, \phi_M) = \text{Re}\left\{ \sum_{\upsilon=0}^{\infty} P_{R\upsilon}^{tot}(\tau, \tau_\rho, \theta_M, \phi_M) e^{i\upsilon\omega' t'} \right\}, \tag{B.2}$$

where

$$P_{R\upsilon}^{tot}(\tau, \tau_\rho, \theta_M, \phi_M) = \iint_{4\pi} A_e(\gamma_R) I_\upsilon^{tot}(\tau, \tau_\rho, \theta_R, \phi_R) \sin \theta_R d\theta_R d\phi_R \tag{B.3}$$

and

$$I_\upsilon^{tot} = I_{d\upsilon} + I_{ri,\upsilon} . \tag{B.4}$$

Note that $\theta = \theta_R$ and $\phi = \phi_R$.

For millimeter waves, the carrier frequency is very large and, therefore, the bandwidth of the received signal is narrow. For such a small bandwidth, the effective aperture and gain of the receiving antenna can be taken to be independent of frequency and to be related by the general expression

$$A_e(\gamma_R) = \frac{\lambda_o^2}{4\pi} D(\gamma_R) ,$$ (B.5)

where λ_o is the free space wavelength and $D(\gamma_R)$ is the directive gain of the antenna at the carrier frequency.

For analytical convenience, the directive gain is assumed to be Gaussian with a narrow beamwidth $\Delta\gamma_M$ and no sidelobes, i.e.,

$$D(\gamma_R) = \left(\frac{2}{\Delta\gamma_M}\right)^2 e^{-(\gamma_R/\Delta\gamma_M)^2} \quad , \quad \Delta\gamma_M << \pi ,$$ (B.6)

which is normalized such that

$$\iint_{4\pi} D(\gamma_R)\sin\theta_R d\theta_R d\phi_R = 4\pi .$$ (B.7)

Using the normalized directive gain $D(\gamma_R)$ in (B.6) and the total intensity expressed as in (B.4), the total received instantaneous power is obtained as the sum of diffuse power $P_{R,d}$ and reduced incident power $P_{R,ri}$. The received diffuse power is obtained as follows

$$P_{R,d}(\tau,\tau_\rho,t',\theta_M,\phi_M) = \mathrm{Re}\left\{\sum_{\upsilon=0}^{\infty} P_{R,d\upsilon}(\tau,\tau_\rho,\theta_M,\phi_M)e^{i\upsilon\omega't'}\right\} ,$$ (B.8)

where

$$P_{R,d\upsilon}(\tau,\tau_\rho,\theta_M,\phi_M) = \iint\limits_{4\pi} A_e(\gamma_R)I_{d\upsilon}(\tau,\tau_\rho,\theta_R,\phi_R)\sin\theta_R d\theta_R d\phi_R$$

$$= \frac{\lambda_o^2}{4\pi}\iint\limits_{4\pi} D(\gamma_R)I_{d\upsilon}(\tau,\tau_\rho,\theta_R,\phi_R)\sin\theta_R d\theta_R d\phi_R$$

$$\cong \frac{\lambda_o^2}{4\pi}I_{d\upsilon}(\tau,\tau_\rho,\theta_M,\phi_M)\iint\limits_{4\pi} D(\gamma_R)\sin\theta_R d\theta_R d\phi_R$$

$$= \lambda_o^2 I_{d\upsilon}(\tau,\tau_\rho,\theta_M,\phi_M) \quad .$$

(B.9)

Similarly, the received reduced incident power is obtained as follows

$$P_{R,ri}(\tau,\tau_\rho,t',\theta_M,\phi_M) = \text{Re}\left\{\sum_{\upsilon=0}^{\infty} P_{R,ri,\upsilon}(\tau,\tau_\rho,\theta_M,\phi_M)e^{i\upsilon\omega't'}\right\}, \tag{B.10}$$

where (using (2.4.1))

$$P_{R,ri,\upsilon}(\tau,\tau_\rho,\theta_M,\phi_M) = \iint\limits_{4\pi} A_e(\gamma_R)I_{ri,\upsilon}(\tau,\tau_\rho,\theta_R,\phi_R)\sin\theta_R d\theta_R d\phi_R$$

$$\approx \frac{\lambda_o^2}{4\pi}S_p f_\upsilon e^{-(\tau_\rho/\sigma_t w)^2}e^{-\eta_\upsilon\tau}\int_0^{2\pi}\int_0^{\pi} D(\gamma_R)\frac{\delta(\theta_R)}{2\pi\sin\theta_R}\sin\theta_R d\theta_R d\phi_R$$

$$= \frac{\lambda_o^2}{4\pi}S_p f_\upsilon e^{-(\tau_\rho/\sigma_t w)^2}e^{-\eta_\upsilon\tau}D(\theta_M) \quad .$$

(B.11)

The instantaneous power is normalized to the received time-averaged power at $\tau=0$, $\tau_\rho=0$, $\theta_M=0$ and $\phi_M=0$, which is given by

$$\langle P_R(0,0,t',0,0)\rangle \equiv \frac{1}{T'}\int_{-T'/2}^{T'/2} P_R(0,0,t',0,0)dt' = \frac{\lambda_o^2}{4\pi}D(0)S_p . \tag{B.12}$$

Thus, the normalized total instantaneous power is the sum of the reduced incident and the diffuse normalized powers, namely,

$$P'(\tau,\tau_\rho,t',\theta_M,\phi_M) = \frac{P(\tau,\tau_\rho,t',\theta_M,\phi_M)}{\langle P_R(0,0,t',0,0)\rangle} = P'_{ri} + P'_d . \tag{B.13}$$

Using the expressions in (B.9) and (B.11), the total normalized instantaneous received power takes the form:

$$P'(\tau,\tau_\rho,t',\theta_M,\phi_M) = \mathrm{Re}\left\{\sum_{\upsilon=0}^{\infty} P'_\upsilon(\tau,\tau_\rho,\theta_M,\phi_M)e^{i\upsilon\omega't'}\right\},$$ (B.14)

where

$$P'_\upsilon(\tau,\tau_\rho,\theta_M,\phi_M) = \frac{D(\theta_M)}{D(0)}e^{-(\tau_\rho/\sigma_r w)^2}f_\upsilon e^{-\eta_\upsilon\tau} + \frac{4\pi}{S_p D(0)}I_{d\upsilon}(\tau,\tau_\rho,\theta_M,\phi_M).$$ (B.15)

The first term in (B. 15) combined with (B.14) yields

$$
\begin{aligned}
P'_{ri} &= \sum_{\upsilon=0}^{\infty} P'_{\upsilon,ri}\\
&= \frac{D(\theta_M)}{D(0)}e^{-(\tau_\rho/\sigma_r w)^2}e^{-\tau}\,\mathrm{Re}\sum_{\upsilon=0}^{\infty}f_\upsilon e^{i\upsilon\omega'(t-\tau)}\\
&= \frac{D(\theta_M)}{D(0)}e^{-(\tau_\rho/\sigma_r w)^2-\tau}f(\tau,t)\qquad\quad,
\end{aligned}
$$ (B.16)

where $$f(\tau,t)=f(t-\tau).$$ (B.16a)

Note that at $\tau = 0$, $\tau_\rho = 0$ and for $\theta_M = 0$,

$$P_{ri}=f(0,t),$$ (B.17)

which is given in(4.1.3) for a Gaussian pulse shape.

REFERENCES

1. A. Ishimaru, *Wave Propagation and Scattering in Random Media,* Vol.1, Academic Press, New York, 1978.

2. A. Ishimaru, "Theory and Application of Wave Propagation and Scattering in Random Media," Proceedings of the IEEE, vol.65, no.7, pp.1030 -1066, July 1977.

3. E. J. Violette, R. H. Espeland, A. R. Mitz, F. A. Goodknight and F. Schwering, "SHF-EHF propagation through vegetation on Colorado east slope," R&D Tech. Rep. CECOM-81-S020-F, Fort Monmouth, NJ, June 1981.

4. E. J. Violette, R. H. Espeland and F. Schwering, "Vegetation loss measurement at 9.6, 28.8 and 57.6 GHz through a pecan tree orchard in Texas," U.S Army R&D Tech. Rep. CEOM-83-2, Fort Monmouth, NJ, March 1983.

5. G. M. Whitman, F. K. Schwering and L. W. Chen, "A theory of millimeter-wave propagation in vegetation," U.S Army Commun.-Electon. Command, R&D Tech. Rep. CECOM-TR-84-5. Fort Monmouth. NJ, July 1984.

6. G. M. Whitman, F. Schwering and J. Yuan, "Chebyshev Method of Solution to the Time-Dependent Transport Equation in Planar Geometry," *Proceedings of the 1985 International Symposium on Antennas and EM Theory,* China Academic Publishers, Beijing, China, pp. 171-177, August 1985.

7. G. M. Whitman, F. Schwering and N. Cho, "Moment Method Solution of the Time Dependent Transport Equation in Planar Geometry," *Proceedings of the 1985 International Symposium on Antennas and Propagation,* Kyoto, Japan, pp. 687-690, August 1985.

8. F. Schwering and R.A. Johnson, "A Transport Theory of Millimeter-wave Propagation in Woods and Forests," *Journal Wave-Material Interaction,* vol.1, no.2, pp.205-235, April 1986.

9. F. K. Schwering, E.J. Violette and R.H. Espeland, "Millimeter-Wave Propagation in Vegetation: Experiment and Theory," IEEE *Transaction Geoscience And Remote Sensing,* vol.26, no.3, pp. 355-367, May 1988.

10. F. T. Ulaby, T.A. Van Deventer, J.R. East, T.F. Haddock and M.E. Coluzzi, "Millimeter-Wave Bistatic Scattering From Ground Vegetation Targets," IEEE *Transaction Geoscience and Remote Sensing,* vol. 26, no. 3, pp.229-243, May 1988.

11. G. M. Whitman, F. Schwering, A. Triolo and N. Cho, "A Transport Theory of Pulse Propagation in a Strongly Forward Scattering Random Medium," IEEE *Transaction on Antenna and Propagation*, vol. 44, no. 1, pp.205-235, January 1996.

12. H W Chang and A. Ishimaru, "Beam wave Propagation and Scattering in Random Media Based on the Radiative Transfer Theory," *Journal of Wave-Material Interaction*, vol. 2, no. 1, pp.41-69, January 1987.

13. M. N. Ozisik, *Radiative Transfer and Interactions with Conductor and Convection*, JohnWiley and Sons, New York, 1973.

14. A. Weinberg and E. Wigner, *The Physical of Neutron Chain Reactions*, pp.273-276 University of Chicago Press, Chicago, Illinois 1958.

15. S. Chandrasekar, *Radiative Transfer*, Oxford University Press, London, 1959; also Dover, New York, 1960.

16. I. S. Gradshteyn and I. M. Ryzhik, *Tables of Integrals, Series, and Products*, Academic Press, New York, 1965.

17. N. N. Llebedev, *Special Functions and Their Applications*, Dover, New York, 1972.